

Article

Age-Related Differences in Thigh Biarticular Agonist–Antagonist Coordination During 50 m Sprinting: A Phase-Specific Analysis of sEMG and Ground Reaction Force Using Phase Mean Comparisons and Linear Mixed-Effects Models

Kanta Yokota ¹  and Hiroyuki Tamaki ^{2,*}

¹ Graduate School of Physical Education, National Institute of Fitness and Sports in Kanoya, Kanoya 891-2311, Japan; m257006@sky.nifs-k.ac.jp or ky1015jump@outlook.jp

² Department of Sports and Life Science, National Institute of Fitness and Sports in Kanoya, Kanoya 891-2311, Japan

* Correspondence: tamaki@nifs-k.ac.jp

Abstract

Background: Age-related differences in neuromuscular coordination during multi-joint tasks are reported, but phase-specific evidence during maximal sprinting is limited. **Aim:** The aim of this study was to investigate phase-specific age differences in agonist–antagonist coordination of the biarticular thigh muscles during 50 m sprinting. **Methods:** Thirty-eight healthy trained track athletes (Adults: $n = 21$, age = 23.32 ± 2.98 years; Adolescents: $n = 17$, age = 13.65 ± 0.76 years) performed maximal 50 m sprints over force plates. Bilateral rectus femoris (RF) and biceps femoris (BF) sEMG and ground reaction forces were recorded; each stride was segmented into seven phases, and an RF–BF co-contraction index (CCI) was calculated per phase. Between-group differences in phase mean CCI were tested ($\alpha = 0.05$) and quantified with Hedges' g . Speed- and frequency-dependent modulation of CCI was evaluated using linear mixed-effects models (LME; random intercepts for participant) with *Frequency* \times Group and *Speed* \times Group interaction terms; ordinary least squares (OLS) fits on stride cycle-level group means were descriptive. Linear and single-breakpoint segmented models were compared using the corrected Akaike information criterion (AICc) and Akaike weights. **Results:** Adolescents showed higher CCI in contact (right: Adults 0.09 ± 0.05 vs. Adolescents 0.13 ± 0.07 , $g = 0.68$; left: Adults 0.08 ± 0.04 vs. Adolescents 0.12 ± 0.06 , $g = 0.84$) and propulsive phases (right: Adults 0.08 ± 0.05 vs. Adolescents 0.13 ± 0.08 , $g = 0.68$; left: Adults 0.07 ± 0.04 vs. Adolescents 0.12 ± 0.07 , $g = 0.84$; $p < 0.05$ for both legs in both phases). LME identified *Frequency* \times Group interactions in the stride cycle (Δ Slope = 0.10, $p < 0.001$) and late swing (Δ Slope = 0.12, $p < 0.05$) and a *Speed* \times Group interaction in mid swing (Δ Slope = 0.01, $p < 0.05$). Mid swing showed a positive CCI–speed/frequency relationship in both groups, whereas across most other phases Adults downregulated CCI as speed/frequency increased while Adolescents tended to increase CCI. Model selection supported phase-dependent single-breakpoint patterns, with breakpoints around 2.19–2.21 Hz and 6.11 – 9.51 m·s^{−1} in Adults and around 2.11 Hz and 7.13 – 7.59 m·s^{−1} in Adolescents. **Conclusions:** Maximal sprinting revealed phase-specific age differences in BF–RF co-contraction and its scaling with speed/frequency, which may help guide age-informed monitoring and training considerations in developing athletes.



Academic Editor: Mark King

Received: 30 January 2026

Revised: 24 February 2026

Accepted: 2 March 2026

Published: 3 March 2026

Copyright: © 2026 by the authors.

Licensee MDPI, Basel, Switzerland.

This article is an open access article

distributed under the terms and

conditions of the [Creative Commons](https://creativecommons.org/licenses/by/4.0/)

[Attribution \(CC BY\)](https://creativecommons.org/licenses/by/4.0/) license.

Keywords: electromyography; muscle activity; co-contraction index; sprint running; age-related difference; neuromuscular coordination; rectus femoris; biceps femoris; ground reaction force

1. Introduction

Surface electromyography (sEMG) enables the visualization and quantification of neuromuscular activity during human movement, allowing the evaluation of coordination strategies between agonist and antagonist muscles (reciprocal activation/coactivation) as well as individual-specific motor control patterns. The co-contraction index (CCI) has been widely used to quantify agonist–antagonist activation patterns during movement [1–3]. In addition, a force plate system provides ground reaction force (GRF) measurements that support phase identification in cyclic tasks, such as sprint running, including not only contact versus swing based on foot contact and toe-off, but also braking versus propulsion within contact. Combining GRF-defined phases with sEMG-based indices allows for a quantitative, phase-specific assessment of neuromuscular coordination during sprint running.

Biomechanical evidence describing phase-dependent joint torques during sprint running has been reported [4,5]. Reports addressing muscle activation patterns during sprinting also exist [3,6–9]. However, few studies have quantitatively analyzed agonist–antagonist coordination using indices such as CCI within a consistent GRF-defined phase framework, nor have they systematically linked these indices to phase-specific external mechanics during sprinting. Therefore, adding quantitative information on agonist–antagonist coordination to established mechanical descriptions (e.g., joint torques) may further improve our understanding of sprint running. Recent advances in wireless, miniaturized sEMG have further enabled quantitative phase-specific analysis of neuromuscular activation during high-speed and complex field-based movements, such as sprinting, thereby accelerating progress in the characterization of neuromuscular control strategies [10].

Evidence from pediatric cohorts spanning childhood to adolescence suggests greater agonist–antagonist coactivation than in adults, particularly during multi-joint dynamic tasks, whereas clear sex differences are not consistently evident [2,11–13]. In adolescents, coactivation may contribute to joint stabilization [14,15] but may also reflect developmental differences in sensorimotor and reflex control that constrain efficient reciprocal inhibition [16]. In parallel, adolescents show lower pre-activation than adults in demanding SSC tasks [17,18], and pre-activation is related to muscle stiffness [19], collectively supporting an age-related shift toward greater feedforward presetting and reduced reliance on feedback during dynamic movements [12,20]. Age-related differences in neuromuscular coordination during sprint running may reflect ongoing maturation of the sensorimotor system. Immature sensitivity of muscle spindles and γ -motoneuron function [16], greater muscle–tendon compliance that can reduce SSC effectiveness and promote greater reliance on feedback control [17], and relatively lower feedforward activity [20] may make pre-activation prior to ground contact less distinct and increase reliance on reactive (feedback-driven) control, potentially promoting higher co-contraction under demanding conditions. A key limitation in the current literature is the adult-centric evidence base for neuromuscular coordination during sprint running; phase-specific coordination in youth athletes remains under-characterized. As a result, practitioners often have little choice but to draw on adult-derived findings when designing training and injury prevention strategies for developing athletes. The present study advances the field by characterizing phase-specific agonist–antagonist coordination during maximal sprinting within a GRF-defined framework and interpreting age-related differences in the context of ongoing maturation of sensorimotor control. Such mechanistic insight provides a rationale for tailoring training and injury prevention strategies to developmental stage rather than applying a one-size-fits-all adult model.

Sprint running is a high-speed cyclic movement that requires precise phase-dependent coordination between agonist and antagonist muscles, whereas rapid repetition can pro-

mote coactivation [15,21–24]. Among the sprint phases, the late swing is a critical preparatory window immediately preceding ground contact, during which the limb is repositioned to set the mechanical conditions of the subsequent contact. This phase is characterized by high hamstring loading [4,5,25–27] and elevated injury risk [28], consistent with the large joint torques and muscle–tendon demands reported around the terminal swing. Importantly, maximal sprint speed has been linked to pre-support limb-repositioning kinematics (e.g., hip extension angular velocity) immediately prior to contact [29], which aligns with the preparatory foot-retraction strategy often termed pawing. Because this pre-activation and repositioning action can influence the braking and propulsion demands during contact, the late swing represents a phase in which performance-related mechanics and injury-relevant tissue loading converge. From a movement analysis perspective, this phase provides a unique window in which neural control strategies can be evaluated independently of direct ground reaction forces, allowing a clearer separation of feedforward control mechanisms. Therefore, evaluating agonist–antagonist coordination during the late swing, together with GRF-defined contact subphases, may provide mechanistic insight into how maturation-related differences in proprioceptive and feedforward control are expressed in adolescent versus adult sprinting [16–18].

The aim of this study was to investigate phase-specific age differences in agonist–antagonist coordination of the biarticular thigh muscles during 50 m sprinting.

We hypothesized that Adolescents would show higher CCI than Adults during the contact phase and late swing phase.

2. Materials and Methods

2.1. Study Design and Setting

This cross-sectional comparative study examined phase-specific age differences in thigh agonist–antagonist coordination during maximal sprinting. Testing was conducted at the SPORTEC Sports Performance Research Center (National Institute of Fitness and Sports in Kanoya, Kanoya, Japan) on a straight 50 m synthetic tartan track instrumented with embedded force plates. Approval was obtained from the research ethics committee of the National Institute of Fitness and Sports in Kanoya (25-1-37). As this was an observational biomechanics study without prospective assignment to any health-related intervention, clinical trial registration was not applicable. A maximal 50 m sprint trial was conducted in this study. The facility comprises 54 plates in total, including 50 plates spanning the runway and four plates positioned at the start line. After a standardized warm-up, each participant completed a 50 m sprint from a two-point start (both feet in contact with the ground). During the sprint, thigh surface electromyography (sEMG) and ground reaction force (GRF) data were acquired simultaneously. All signals were time-synchronized to allow for precise alignment between neuromuscular and biomechanical measurements. Neuromuscular data were obtained under the mobile-receiver condition (MRC), which we previously described as enabling stable, uninterrupted wireless transmission throughout overground sprinting [10].

2.2. Participants and Recruitment

Standing height and body mass were measured using a body composition analyzer with an integrated manual stadiometer (DC-217A; TANITA, Tokyo, Japan). Body mass was recorded in 0.1 kg increments. Twenty-one adult athletes (twenty males, one female) and seventeen adolescent athletes (seven males, ten females) participated in this study. Participants were recruited by convenience sampling in Kagoshima Prefecture, Japan. All participants were track-and-field athletes (sprint, jump, and middle-distance events) and were registered with the Japan Association of Athletics Federations (JAAF). Adolescents

were junior high school students (13–15 years) recruited from community track-and-field clubs in Kanoya City and Osaki Town. They had 2–5 years of athletics experience and underwent regular sprint training at least twice per week (typically two to four sessions per week). Adults (20–31 years) were university students and working adults recruited locally in Kagoshima Prefecture. None of the participants had competed at the international level; competitive experience ranged from regional (Kagoshima/Kyushu) to national-level competitions. Participants were screened for eligibility prior to testing. Inclusion criteria were no history of neurological disorders and no lower-limb musculoskeletal injury prior to testing. All recruited participants met the eligibility criteria; therefore, no participants were excluded after screening, and all were included in the final analyses. Written informed consent was obtained prior to participation. For adults, the consent form was signed by the participants themselves. For adolescents, written informed consent was signed by their legal guardians, and written assent was also obtained from the adolescents (Figure 1).

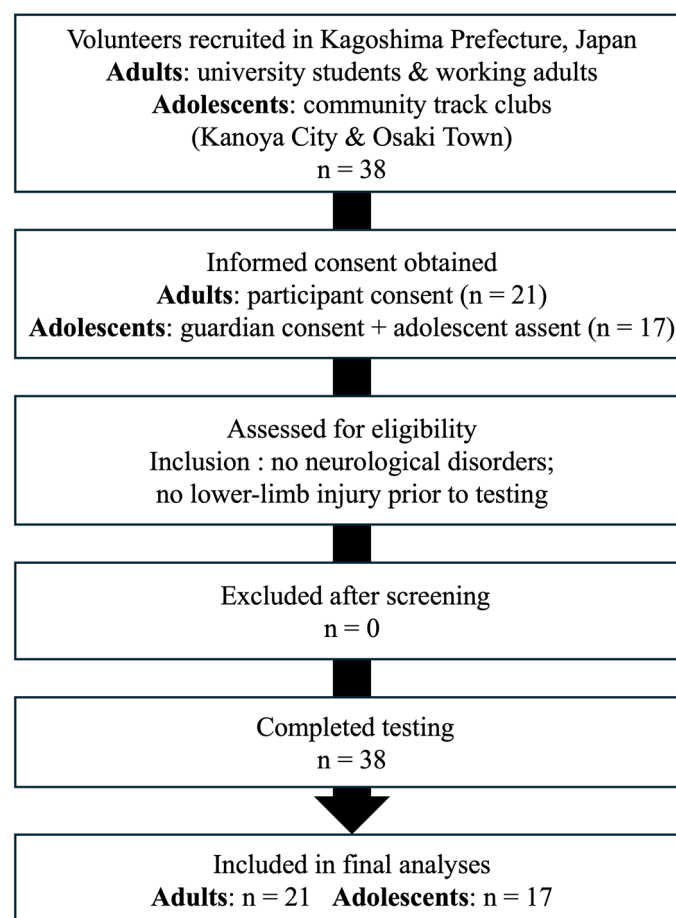


Figure 1. Participant flow diagram. Written informed consent was obtained from adults, and guardian consent plus adolescent assent was obtained for adolescents. No participants were excluded after eligibility screening, and all recruited participants were included in the final analyses.

2.3. Instrumentation and Data Collection

To enable continuous EMG recording during high-speed sprinting, a wireless surface EMG system was used (Cometa Pico EMG, Cometa Systems, Milan, Italy). The sensor mass was approximately 7 g, and no participant reported discomfort or perceived performance impairment during the test. Each sensor unit contained an integrated transmitter and communicated with a common receiver via Bluetooth transmission. Surface EMG was recorded bilaterally from the rectus femoris (RF) and biceps femoris (BF), which constitute a primary agonist–antagonist muscle pair at the thigh, to enable a phase-specific analysis

of co-contraction during sprint running. To improve the signal quality and reduce the skin–electrode impedance, the skin surface was treated before electrode attachment. When necessary, hair was removed, followed by gentle abrasion and cleansing with alcohol.

Surface EMG was recorded using disposable Ag/AgCl electrodes (8 mm diameter; Cardinal Health, Dublin, OH, USA) arranged in a bipolar configuration over the muscle bellies. Electrode placement was guided by the SENIAM recommendations to ensure consistency across participants and muscles [30]. The interelectrode distance was set to approximately 20 mm. The EMG signals were amplified, band-pass filtered (10–500 Hz), and sampled at 2000 Hz. For EMG normalization, maximal voluntary contractions (MVC) were obtained during unilateral isometric contractions. MVC for the RF were performed in a seated position with the hip joint angle set to 90° and the knee joint angle set to 180° (full extension), whereas MVC for the BF were performed in a prone position with the hip joint angle set to 180° (neutral extension) and the knee joint angle set to 90° (flexion). EMG amplitudes during sprinting were then expressed relative to the corresponding MVC. This sampling rate was selected to capture the rapid fluctuations associated with ballistic muscle actions during sprinting and to reduce the risk of signal aliasing. Although the effective frequency content of surface EMG is typically below 500 Hz, oversampling improves signal reconstruction and reliability. This approach is consistent with recommendations for surface EMG analysis and with previous sprint EMG studies [7–10]. In addition, sampling at a rate well above twice the highest frequency of interest conforms to the standard practice for reliable reconstruction and robust timing analyses [14].

GRF data were collected at 2000 Hz using a 50 m force plate system (TF-90100, TF-3055, TF-32120; Tec Gihan, Kyoto, Japan) to identify sprint phases and contact subphases for biomechanical analysis. Data were recorded in “All-Plate Mode,” in which the 50 plates installed along the runway were CPU-integrated to operate as a single continuous force platform (1 m × 50 m). The four plates located at the start line, which were used to distinguish left and right GRF at the instant of start, were not included in the present analyses.

Synchronization between the sEMG and GRF signals was achieved using a transistor–transistor logic (TTL) trigger delivered via a Bayonet Neill–Concelman (BNC) connection. sEMG signals were acquired using a Wave Plus receiver and transferred to a PC via USB using the manufacturer’s software (EMG and Motion Tools, 8.6.2.0; Cometa Systems, Milan, Italy). To accommodate overground sprinting, the receiver was carried by an examiner who followed the participants during the run. Because the receiver was powered through the USB connection, a 30 m active USB extension cable with a built-in signal repeater (KB-USB-R230; Sanwa Supply, Okayama, Japan) was used to avoid signal attenuation over long distances. The Wave Plus receiver supported external synchronization through a 2.5 mm audio jack. A TTL pulse was generated using a starting pistol and delivered simultaneously to the Wave Plus (Cometa Systems, Milan, Italy) and GRF acquisition systems (TF-90100, TF-3055, TF-32120; Tec Gihan, Kyoto, Japan) via a 2.5 mm jack-to-BNC cable to ensure accurate temporal alignment.

2.4. Data Analysis

sEMG and GRF data were analyzed using MATLAB (R2023a; MathWorks, Natick, MA, USA).

The sEMG signals were processed in four steps as follows. First, the signals were band-pass filtered (20–500 Hz). Second, they were full-wave rectified. Third, the rectified signals were smoothed using a 0.03 s time constant. Fourth, the amplitudes were normalized to the peak value obtained during maximal voluntary contraction (MVC).

Neuromuscular coordination was quantified using the co-contraction index (CCI) [1]:

$$\text{CCI} = (\text{LEMG}/\text{HEMG}) \times (\text{LEMG} + \text{HEMG}), \quad (1)$$

where LEMG is the lower, HEMG is the higher normalized sEMG amplitudes, respectively, between the RF and BF. With EMG normalized to MVC (0–1), this CCI ranges from 0 to 2 [3,31,32]. We note that other commonly used CCI formulations (e.g., Falconer & Winter) scale from 0 to 1, and methodological work has highlighted that the choice of CCI formulation (e.g., Rudolph vs. Falconer & Winter) can influence the resulting CCI values and their interpretation [33]. Because ratio-based formulations can yield high values when the two opposing EMG signals are similar even at low magnitudes, they may inflate CCI during low-activation intervals in cyclic tasks [33]. Therefore, we adopted the Rudolph-type CCI to maintain methodological consistency with prior sprinting studies assessing RF–BF co-contraction using a similar antagonist biarticular pair and high-speed task demands [3]. The phase-specific CCI was computed.

GRF and center of pressure (COP) processing and event detection were performed as described in our previous study [10] without modification. Briefly, GRF signals were low-pass filtered at 50 Hz, and foot strike and foot-off were identified from the vertical GRF (Fz) using a 20 N threshold sustained for 20 consecutive samples. Ground contact was defined as the interval from foot strike to foot-off, and its duration was defined as contact time. A stride cycle was defined as the interval from ipsilateral foot-off to the subsequent ipsilateral foot strike, and its duration was defined as stride cycle time.

In the present study, ground contact was additionally subdivided into braking and propulsion using the anteroposterior GRF (Fy): braking and propulsion were defined as the intervals before and after the Fy zero-crossing (sign change), respectively. Braking and propulsive times were computed as the durations of the braking and propulsion intervals, respectively. In addition to absolute durations, braking and propulsive times were normalized to the contact time and expressed as percentages of the contact time (i.e., contact time = 100%). The stride cycle was subdivided into early-, mid-, and late-swing phases, yielding a total of seven phases (Figures 2 and 3).

Stride cycle length and temporal variables were derived from the anteroposterior COP. For each stride cycle, the midpoint of the ipsilateral ground-contact interval was identified, and a representative COP position was obtained by averaging 10 samples centered on this midpoint (± 5 samples). Stride cycle length was defined as the distance between the COP positions at successive ipsilateral foot strikes. Stride cycle frequency was calculated as the reciprocal of the stride cycle time, and the stride cycle speed was obtained by multiplying the stride cycle length by the stride cycle frequency.

2.5. Statistical Analysis

Statistical analyses were performed using MATLAB (R2023a; The MathWorks, Natick, MA, USA). Data are presented as mean \pm standard deviation (SD). The reliability of the Cometa Pico sEMG system used in the present study has been reported previously (ICC = 0.964) [10].

For the phase mean analysis, a representative CCI value was computed for each participant by averaging the CCI across all available stride cycles within each phase. Between-group differences in the phase mean CCI were tested separately for each phase using Welch's two-sample *t*-test, which does not assume equal variances and is relatively robust to moderate deviations from normality. Effect sizes were quantified using Hedges' *g*. Statistical significance was set at $\alpha = 0.05$. Within each group, left–right differences were evaluated separately for each phase using paired-sample *t*-tests on participant-level phase mean values (i.e., the within-participant mean across all available cycles for a given phase).

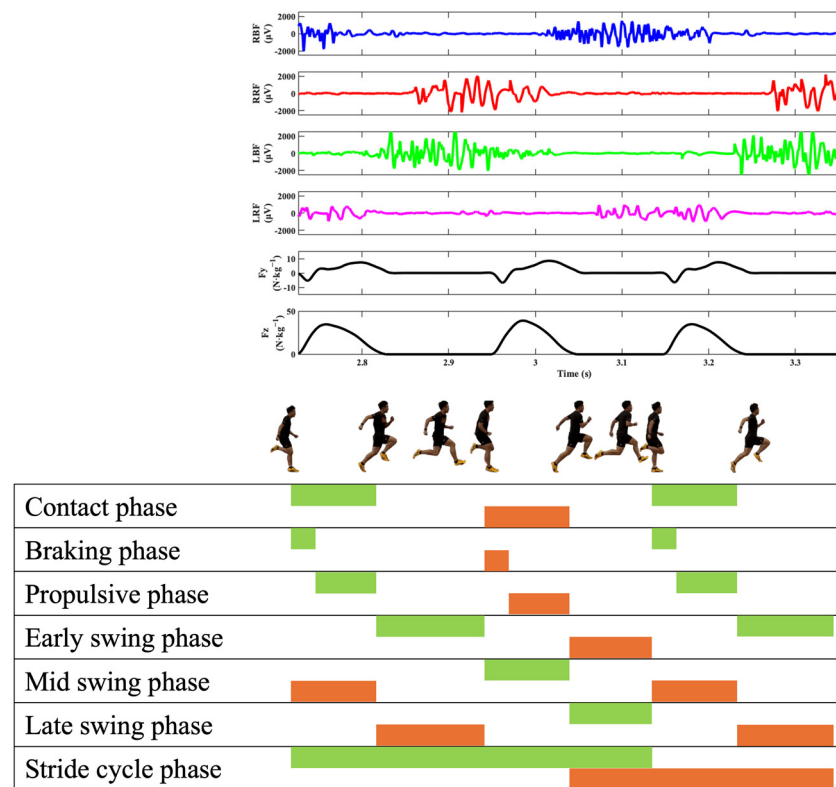


Figure 2. Representative recordings of sEMG (RBF, right leg biceps femoris, blue line; RRF, right leg rectus femoris, red line; LBF, left leg biceps femoris, green line; LRF, left leg rectus femoris, pink line) and ground reaction forces (F_y , anterior–posterior, black line; F_z , vertical, black line) obtained from an Adult participant during the 50 m sprint. The middle panel shows sequential photographs corresponding to the analyzed phases. The bottom panel summarizes the phase definitions and the color-coded phase segments (right leg: green; left leg: orange).

To test whether the association between the explanatory variable and CCI differed between groups while accounting for repeated observations within participants, linear mixed-effects models (LME) were fitted separately for the stride cycle frequency and stride cycle speed. The model was specified as follows:

$$CCI \sim x \times \text{Group} + (x | \text{participant}), \tag{2}$$

where x denotes the explanatory variable (stride cycle frequency or stride cycle speed), group indicates Adults or Adolescents, and participant-level random intercepts and random slopes were included. Between-group differences in x -related modulation of CCI were evaluated using the $x \times \text{group}$ interaction term. For visualization, fitted regression lines and 95% confidence intervals were derived from the fixed-effect predictions of the LME (i.e., excluding random effects). For each phase-specific linear mixed-effects model, assumptions were assessed using residual-vs-fitted and normal Q–Q plots.

In addition, to summarize overall group-level trends based on stride-cycle-averaged data, ordinary least squares (OLS) regression was applied to group mean points obtained by averaging across participants at each stride cycle. Because these group mean points do not retain participant-level information, OLS results were treated as descriptive only and were not used for primary inferences.

To examine whether a threshold-like change in the relationships of stride cycle frequency and speed with CCI was supported at the group level, an Akaike information criterion with small-sample correction (AICc) model comparison was performed separately for each group using step-averaged group mean points. For each explanatory variable

(stride cycle frequency and stride cycle speed), the candidate models included (1) a simple linear model, and (2) a segmented (piecewise) linear model with a single breakpoint. The breakpoint location was selected as the value that minimized AICc within the observed range of the explanatory variable. Model support was judged by $\Delta AICc$ (relative to the best model) and the corresponding Akaike weights, with larger support indicating a better balance of goodness-of-fit and parsimony. The AICc procedure was used to characterize whether a threshold was supported within each group and was not used as the primary inferential test of between-group differences.

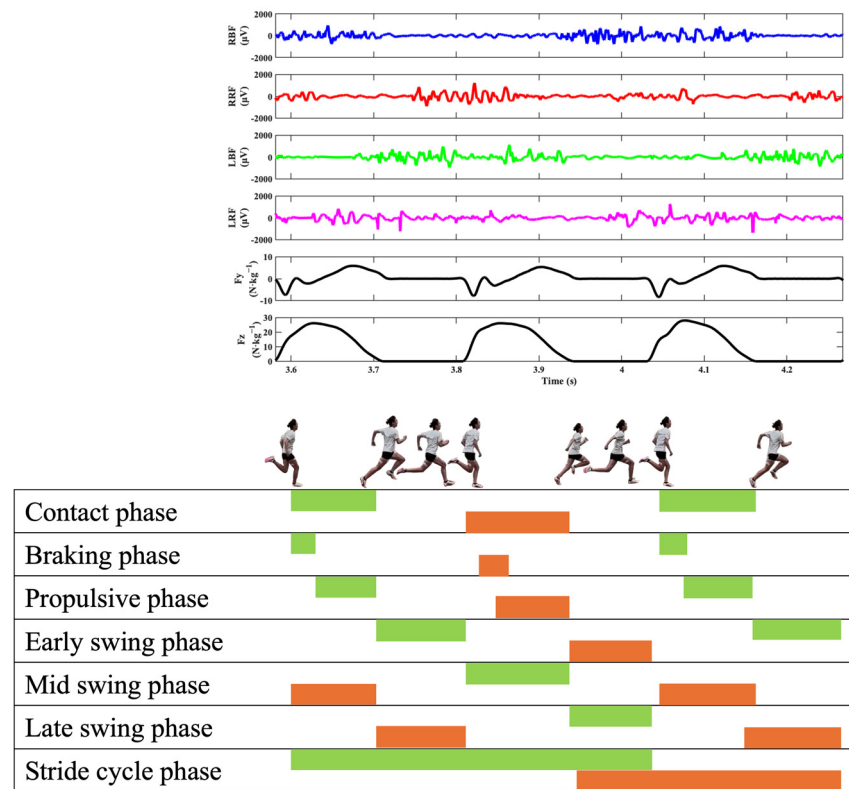


Figure 3. Representative recordings of sEMG (RBF, right leg biceps femoris, blue line; RRF, right leg rectus femoris, red line; LBF, left leg biceps femoris, green line; LRF, left leg rectus femoris, pink line) and ground reaction forces (Fy, anterior–posterior, black line; Fz, vertical, black line) obtained from an Adolescent participant during the 50 m sprint. The middle panel shows sequential photographs corresponding to the analyzed phases. The bottom panel summarizes the phase definitions and the color-coded phase segments (right leg: green; left leg: orange).

3. Results

3.1. Participants Characteristics

Twenty-one adult athletes (twenty males: 23.5 ± 3.0 years, 1.73 ± 0.06 m, 69.6 ± 7.9 kg, one female: 20 years, 1.58 m, 51.4 kg) and seventeen adolescent athletes (seven males: 13.6 ± 0.7 years, 1.63 ± 0.04 m, 48.4 ± 5.8 kg, ten females: 13.7 ± 0.8 years, 1.58 ± 0.03 m, 47.5 ± 3.1 kg) participated in this study. The participant characteristics are summarized in Table 1. The Adult group consisted of university students and working adults, while the Adolescent group comprised junior high school students.

3.2. Neuromuscular Coordination During Sprinting

Phase-specific BF–RF co-contraction index (CCI) values during sprinting differed between Adults and Adolescents (Figure 4). Group comparisons were based on participant-level phase mean CCI values averaged across all available ipsilateral stride cycles for each

leg. Adults exhibited lower CCI than Adolescents in the contact phase for both legs (right: $p < 0.05$, $g = 0.68$; left: $p < 0.05$, $g = 0.84$) and in the propulsive phase for both legs (right: $p < 0.05$, $g = 0.76$; left: $p < 0.05$, $g = 0.89$). Detailed values are provided in Table 2. No significant between-group differences were observed in swing-related phases. Within each group, no significant left–right differences were detected within the same phase (Table 3).

Table 1. Participant characteristics by group.

Group Name		Height (m)	Body Mass (kg)	Age (yr)	Age Range (yr)
Adults <i>n</i> = 21	mean	1.72	68.74	23.32	20~31
	SD	0.07	8.61	2.98	
Adolescents <i>n</i> = 17	mean	1.60	47.86	13.65	13~15
	SD	0.04	4.42	0.76	

Table 2. Phase mean BF–RF co-contraction index (CCI) for each leg across phases in Adults and Adolescents.

Leg Name	Phase Name	Adults	Adolescents	<i>p</i> Value	Effect Size (<i>g</i>)
Right	Stride cycle	0.08 ± 0.04	0.09 ± 0.03	$p > 0.05$	0.34
	Mid swing	0.10 ± 0.05	0.11 ± 0.04	$p > 0.05$	0.14
	Early swing	0.08 ± 0.05	0.08 ± 0.03	$p > 0.05$	0.07
	Late swing	0.07 ± 0.04	0.08 ± 0.04	$p > 0.05$	0.36
	Contact	0.09 ± 0.05	0.13 ± 0.07	$p < 0.05$	0.68
	Braking	0.09 ± 0.06	0.12 ± 0.07	$p > 0.05$	0.36
	Propulsive	0.08 ± 0.05	0.13 ± 0.08	$p < 0.05$	0.76
Left	Stride cycle	0.08 ± 0.03	0.09 ± 0.03	$p > 0.05$	0.45
	Mid swing	0.10 ± 0.05	0.11 ± 0.05	$p > 0.05$	0.22
	Early swing	0.07 ± 0.04	0.08 ± 0.03	$p > 0.05$	0.31
	Late swing	0.06 ± 0.03	0.08 ± 0.04	$p > 0.05$	0.52
	Contact	0.08 ± 0.04	0.12 ± 0.06	$p < 0.05$	0.84
	Braking	0.08 ± 0.05	0.11 ± 0.07	$p > 0.05$	0.54
	Propulsive	0.07 ± 0.04	0.12 ± 0.07	$p < 0.05$	0.89

Values are mean ± SD. *p* values are from Welch’s two-sample *t*-test (unequal variances). Effect size is Hedges’ *g*.

Table 3. Within-group left–right differences in phase mean BF–RF CCI.

Group Name	Phase Name	Left Leg	Right Leg	<i>p</i> Value
Adults	Stride cycle	0.08 ± 0.03	0.08 ± 0.04	$p > 0.05$
	Mid swing	0.10 ± 0.05	0.10 ± 0.05	$p > 0.05$
	Early swing	0.07 ± 0.04	0.08 ± 0.05	$p > 0.05$
	Late swing	0.06 ± 0.03	0.07 ± 0.04	$p > 0.05$
	Contact	0.08 ± 0.04	0.09 ± 0.05	$p > 0.05$
	Braking	0.08 ± 0.05	0.09 ± 0.06	$p > 0.05$
	Propulsive	0.07 ± 0.04	0.08 ± 0.05	$p > 0.05$
Adolescents	Stride cycle	0.09 ± 0.03	0.09 ± 0.03	$p > 0.05$
	Mid swing	0.11 ± 0.05	0.11 ± 0.04	$p > 0.05$
	Early swing	0.08 ± 0.03	0.08 ± 0.03	$p > 0.05$
	Late swing	0.08 ± 0.04	0.08 ± 0.04	$p > 0.05$
	Contact	0.12 ± 0.06	0.13 ± 0.07	$p > 0.05$
	Braking	0.11 ± 0.07	0.11 ± 0.07	$p > 0.05$
	Propulsive	0.12 ± 0.07	0.13 ± 0.08	$p > 0.05$

Values are mean ± SD. *p* values are from Welch’s two-sample *t*-test (unequal variances). Effect size is Hedges’ *g*.

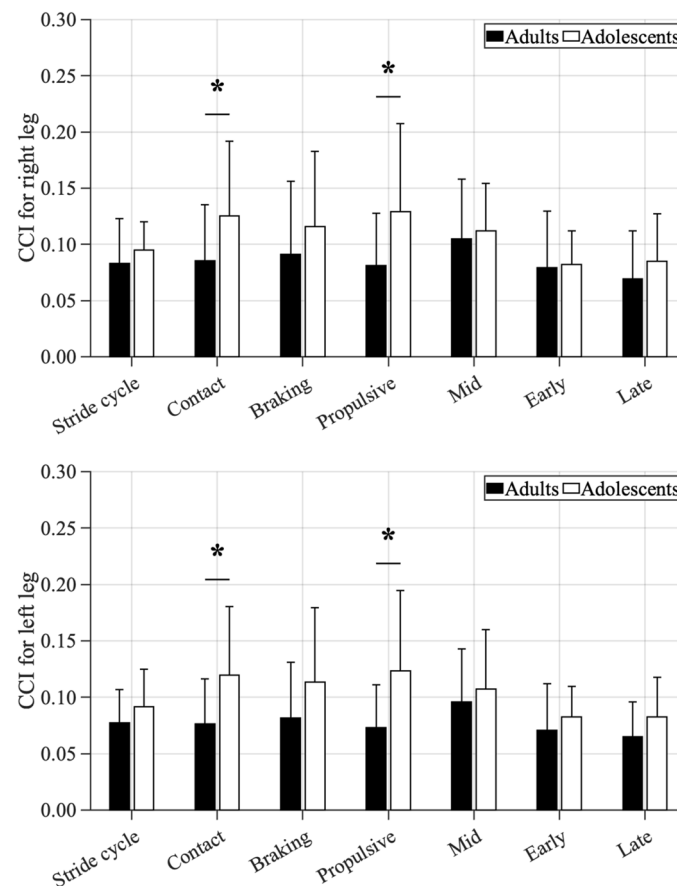


Figure 4. Phase mean BF–RF co-contraction index (CCI) across the seven phases for the right (upper panel) and left (lower panel) leg during the 50 m sprint. CCI was computed for each ipsilateral stride cycle and averaged across all available cycles within each phase for each participant. Bars indicate group means (Adults: black; Adolescents: white), and error bar represent standard deviation. Between-group differences were assessed for each phase using Welch’s two-sample *t*-test. * indicates $p < 0.05$.

3.3. Relationship Between Neuromuscular Coordination and Sprint Performance Variables

3.3.1. Linear Mixed-Effects Models Analysis

Group differences in the CCI–frequency and CCI–speed relationships were assessed using the corresponding interaction terms (Frequency \times Group and Speed \times Group). The Frequency \times Group interaction was significant in the stride cycle phase ($p < 0.001$) and the late swing phase ($p < 0.05$), indicating that the slope of the CCI–frequency relationship differed between groups in these phases (Figure 5). Specifically, in the stride cycle phase, the fixed-effect slope was 0.00 (95% CI: -0.04 to 0.04) in Adults and 0.10 (95% CI: 0.06 to 0.15) in Adolescents, yielding a between-group difference of $|\Delta Slope|$ (Adults – Adolescents) = -0.10 (95% CI: -0.16 to -0.04). In the late swing phase, the corresponding slopes were -0.04 (95% CI: -0.11 to 0.03) in Adults and 0.08 (95% CI: 0.01 to 0.16) in Adolescents, yielding a between-group difference of $|\Delta Slope|$ (Adults – Adolescents) = 0.12 (95% CI: 0.02 to 0.22). In addition, the Speed \times Group interaction was significant in the mid swing phase ($p < 0.05$), demonstrating a between-group difference in the slope of the CCI–speed relationship during mid swing (Figure 6). In this phase, the fixed-effect slope was 0.00 (95% CI: 0.00 to 0.01) in Adults and 0.01 (95% CI: 0.01 to 0.02) in Adolescents, yielding a between-group difference of $|\Delta Slope|$ (Adults – Adolescents) = 0.01 (95% CI: 0.00 to 0.01). The fixed-effect slopes for each group, the estimated slope differences ($|\Delta Slope|$), and their 95% confidence intervals for each phase are summarized in Tables 4 and 5.

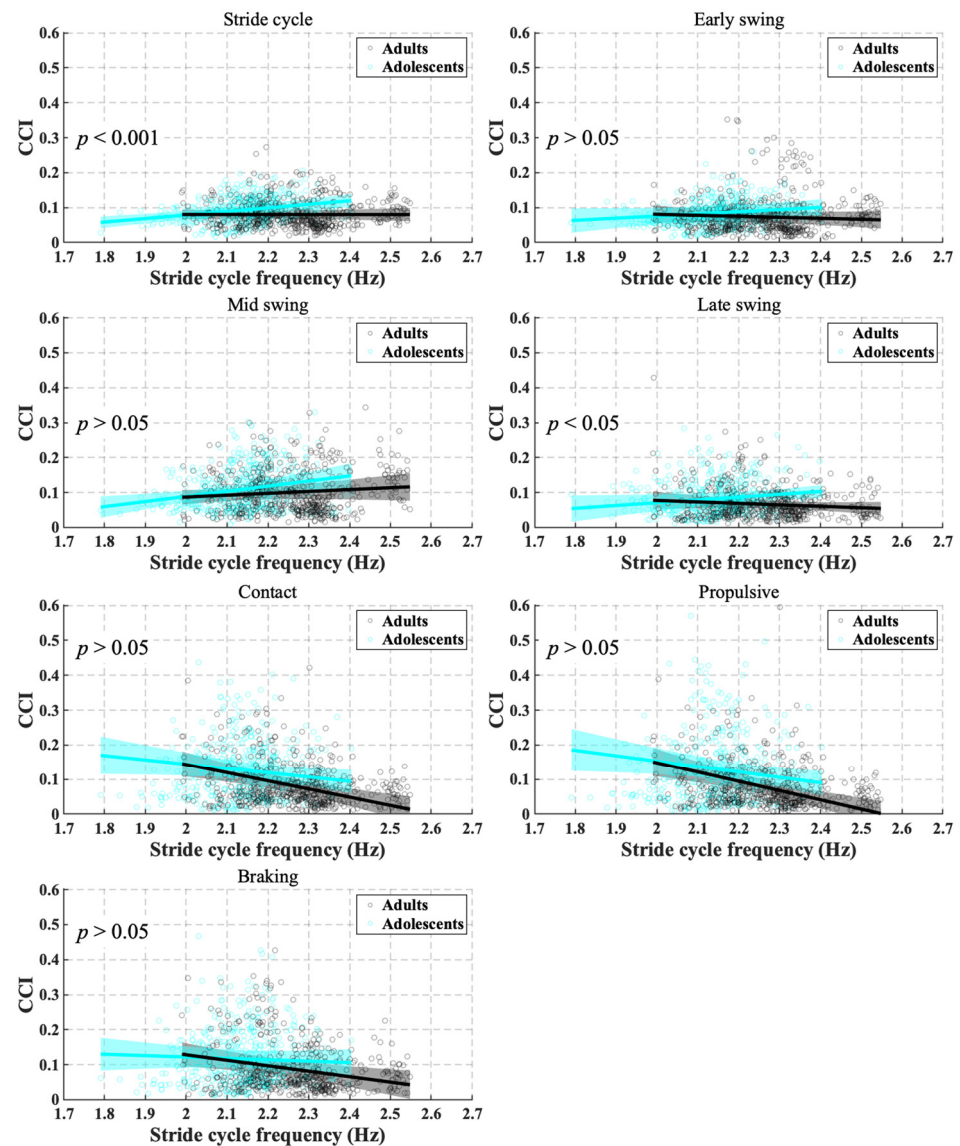


Figure 5. Relationship between stride cycle frequency and BF–RF co-contraction index (CCI) across seven phases (stride cycle, early swing, mid swing, late swing, contact, braking, and propulsive), estimated using linear mixed-effects models (LME). Points represent observed phase-specific CCI values for individual stride cycles (multiple observations per participant). Solid lines show fixed-effect predictions for Adults (gray) and Adolescents (cyan), and shaded bands indicate 95% confidence intervals. p -values shown in each panel correspond to the *Frequency* \times *Group* interaction term (between-group difference in the frequency–CCI association). Statistical significance was set at $p < 0.05$.

3.3.2. Ordinary Least Squares Analysis

To complement the participant-level LME results, we additionally examined descriptive group-level trends using OLS regression. For descriptive group-level trends based on group mean points, between-group differences in slopes were evaluated using the interaction terms (*Frequency* \times *Group* and *Speed* \times *Group*) in OLS models. For frequency, significant slope differences between groups were observed in the late swing ($p < 0.001$), stride cycle ($p < 0.05$), contact ($p < 0.001$), braking ($p < 0.01$), and propulsive phases ($p < 0.001$) (Figure 7). For speed, significant slope differences were detected in the early swing ($p < 0.01$), mid swing ($p < 0.01$), and propulsive phases ($p < 0.05$) (Figure 8). The corresponding regression coefficients, slope differences ($|\Delta Slope|$), and 95% confidence intervals are summarized in Tables 6 and 7.

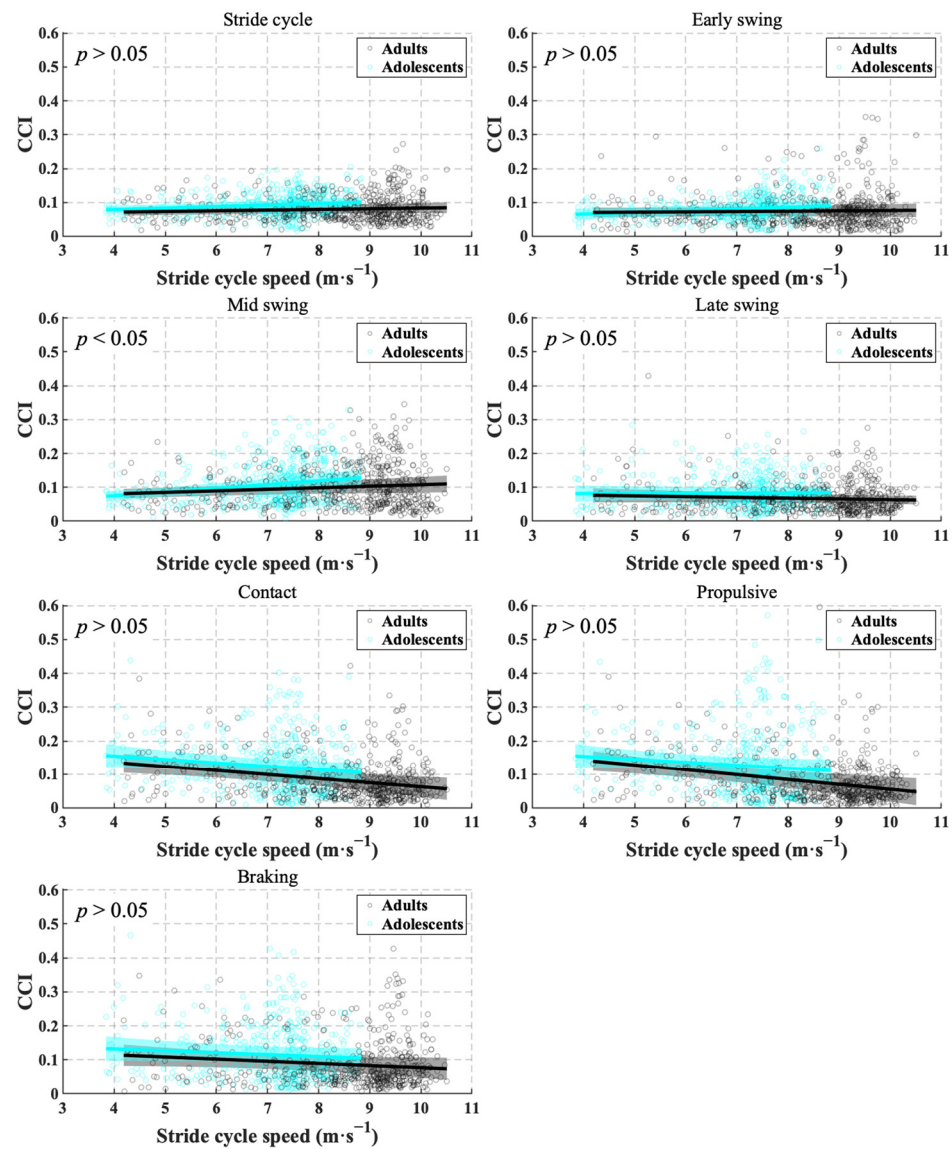


Figure 6. Relationship between stride cycle speed and BF–RF co-contraction index (CCI) across seven phases (stride cycle, early swing, mid swing, late swing, contact, braking, and propulsive), estimated using linear mixed-effects models (LME). Points represent observed phase-specific CCI values for individual stride cycles (multiple observations per participant). Solid lines show fixed-effect predictions for Adults (gray) and Adolescents (cyan), and shaded bands indicate 95% confidence intervals. *p*-values shown in each panel correspond to the *Speed* × *Group* interaction term (between-group difference in the speed–CCI association). Statistical significance was set at *p* < 0.05.

Table 4. Linear mixed-effects model (LME) results for the association between stride cycle frequency and BF–RF co-contraction index (CCI) across phases.

Phase Name	Adults Slope [95% CI]	Adolescents Slope [95% CI]	ΔSlope [95% CI]	<i>p</i> (<i>Frequency</i> × <i>Group</i>)
Stride cycle	0.00 [−0.04, 0.04]	0.10 [0.06, 0.15]	0.10 [0.04, 0.16]	<i>p</i> < 0.001
Early swing	−0.03 [−0.10, 0.04]	0.06 [−0.01, 0.13]	0.09 [−0.01, 0.19]	<i>p</i> > 0.05
Mid swing	0.05 [−0.03, 0.14]	0.15 [0.05, 0.24]	0.09 [−0.04, 0.22]	<i>p</i> > 0.05
Late swing	−0.04 [−0.11, 0.03]	0.08 [0.01, 0.16]	0.12 [0.02, 0.22]	<i>p</i> < 0.05

Table 4. Cont.

Phase Name	Adults Slope [95% CI]	Adolescents Slope [95% CI]	$ \Delta Slope $ [95% CI]	<i>p</i> (Frequency × Group)
Contact	−0.24 [−0.35, −0.13]	−0.12 [−0.24, −0.00]	0.11 [−0.05, 0.27]	<i>p</i> > 0.05
Braking	−0.16 [−0.26, −0.05]	−0.04 [−0.15, 0.07]	0.12 [−0.04, 0.27]	<i>p</i> > 0.05
Propulsive	−0.27 [−0.38, −0.15]	−0.16 [−0.29, −0.03]	0.11 [−0.06, 0.28]	<i>p</i> > 0.05

Slopes and 95% confidence intervals (CI) are derived from fixed effects. $|\Delta Slope|$ denotes the between-group difference in slopes (Adults − Adolescents). *p*-values correspond to the Frequency × Group interaction term.

Table 5. Linear mixed-effects model (LME) results for the association between (stride cycle speed and BF–RF co-contraction index (CCI) across phases.

Phase Name	Adults Slope [95% CI]	Adolescents Slope [95% CI]	$ \Delta Slope $ [95% CI]	<i>p</i> (Speed × Group)
Stride cycle	0.00 [0.00, 0.00]	0.00 [0.00, 0.01]	0.00 [0.00, 0.01]	<i>p</i> > 0.05
Early swing	0.00 [0.00, 0.00]	0.01 [0.00, 0.01]	0.00 [0.00, 0.01]	<i>p</i> > 0.05
Mid swing	0.00 [0.00, 0.01]	0.01 [0.01, 0.02]	0.01 [0.00, 0.01]	<i>p</i> < 0.05
Late swing	0.00 [−0.01, 0.00]	0.00 [0.00, 0.01]	0.00 [0.00, 0.00]	<i>p</i> > 0.05
Contact	−0.01 [−0.02, −0.01]	−0.01 [−0.02, −0.01]	0.00 [−0.01, 0.01]	<i>p</i> > 0.05
Braking	−0.01 [−0.01, 0.00]	−0.01 [−0.01, 0.00]	0.00 [−0.01, 0.01]	<i>p</i> > 0.05
Propulsive	−0.02 [−0.02, −0.01]	−0.01 [−0.02, 0.00]	0.01 [−0.01, 0.02]	<i>p</i> > 0.05

Slopes and 95% confidence intervals (CI) are derived from fixed effects. $|\Delta Slope|$ denotes the between-group difference in slopes (Adults − Adolescents). *p*-values correspond to the Speed × Group interaction term.

Table 6. Slopes and 95% CIs are from ordinary least squares (OLS) models fitted to phase-specific group mean values at each stride cycle.

Phase Name	Adults Slope [95% CI]	Adolescents Slope [95% CI]	$ \Delta Slope $ [95% CI]	<i>p</i> (Slope Difference; Frequency × Group)
Stride cycle	0.06 [−0.01, 0.12]	0.15 [0.09, 0.21]	0.10 [0.01, 0.18]	<i>p</i> < 0.05
Early swing	0.05 [−0.03, 0.13]	0.07 [−0.01, 0.15]	0.02 [−0.09, 0.13]	<i>p</i> > 0.05
Mid swing	0.20 [0.07, 0.33]	0.32 [0.20, 0.45]	0.12 [−0.06, 0.30]	<i>p</i> > 0.05
Late swing	−0.12 [−0.20, −0.05]	0.10 [0.03, 0.17]	0.22 [0.12, 0.33]	<i>p</i> < 0.01
Contact	−0.53 [−0.66, −0.39]	−0.15 [−0.28, −0.02]	0.38 [0.19, 0.57]	<i>p</i> < 0.001
Braking	−0.27 [−0.42, −0.13]	−0.01 [−0.14, 0.12]	0.26 [0.07, 0.46]	<i>p</i> < 0.01
Propulsive	−0.62 [−0.78, −0.45]	−0.17 [−0.33, −0.02]	0.44 [0.22, 0.70]	<i>p</i> < 0.001

The *p*-value corresponds to the Frequency × Group interaction term (between-group difference in slope). $|\Delta Slope| = \text{Adults} - \text{Adolescents}$.

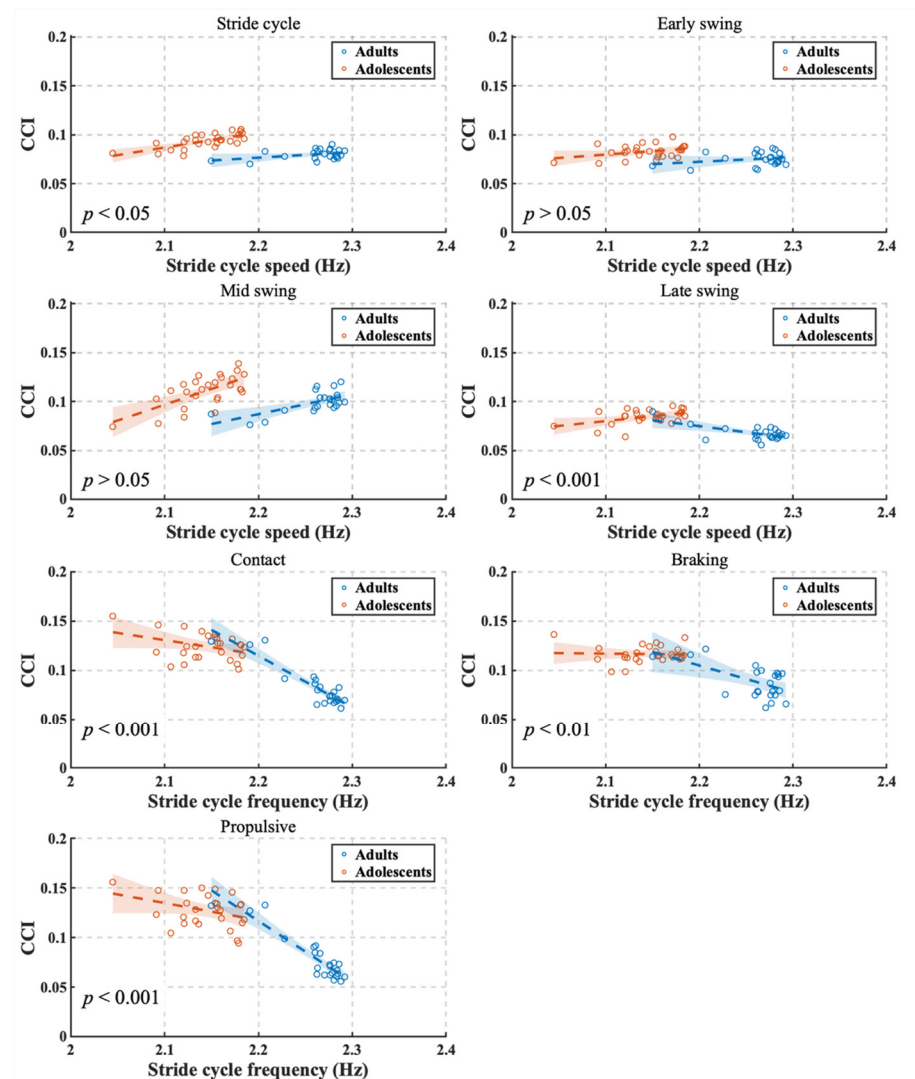


Figure 7. Relationship between stride cycle frequency and BF–RF co-contraction index (CCI) across seven phases (stride cycle, early swing, mid swing, late swing, contact, braking, and propulsive) is shown using ordinary least squares (OLS) regression fitted to group mean values at each stride cycle. Points represent stride cycle-wise group mean values (averaged across participants) for both stride cycle frequency (x) and CCI (y), and dotted lines show OLS fits with 95% confidence bands (color shaded bands).

Table 7. Slopes and 95% CIs are from ordinary least squares (OLS) models fitted to phase-specific group mean values at each stride cycle.

Phase Name	Adults Slope [95% CI]	Adolescents Slope [95% CI]	$ \Delta Slope $ [95% CI]	p (Slope Difference; Speed \times Group)
Stride cycle	0.00 [−0.00, 0.00]	0.00 [0.00, 0.01]	0.00 [−0.00, 0.01]	$p > 0.05$
Early swing	0.00 [−0.00, 0.00]	0.01 [0.00, 0.01]	0.00 [0.00, 0.01]	$p < 0.01$
Mid swing	0.01 [0.00, 0.01]	0.01 [0.01, 0.02]	0.01 [0.00, 0.01]	$p < 0.01$
Late swing	−0.00 [−0.00, 0.00]	0.00 [−0.00, 0.00]	0.00 [−0.00, 0.01]	$p > 0.05$
Contact	−0.01 [−0.02, −0.01]	−0.01 [−0.01, −0.01]	0.00 [−0.00, 0.01]	$p > 0.05$

Table 7. Cont.

Phase Name	Adults Slope [95% CI]	Adolescents Slope [95% CI]	$ \Delta Slope $ [95% CI]	p (Slope Difference; $Speed \times Group$)
Braking	-0.01 [-0.01, -0.00]	-0.00 [-0.01, 0.00]	0.00 [-0.00, 0.01]	$p > 0.05$
Propulsive	-0.02 [-0.02, -0.01]	-0.01 [-0.01, -0.00]	0.01 [0.00, 0.01]	$p < 0.05$

The p -value corresponds to the $Speed \times Group$ interaction term (between-group difference in slope). $|\Delta Slope| = Adults - Adolescents$.

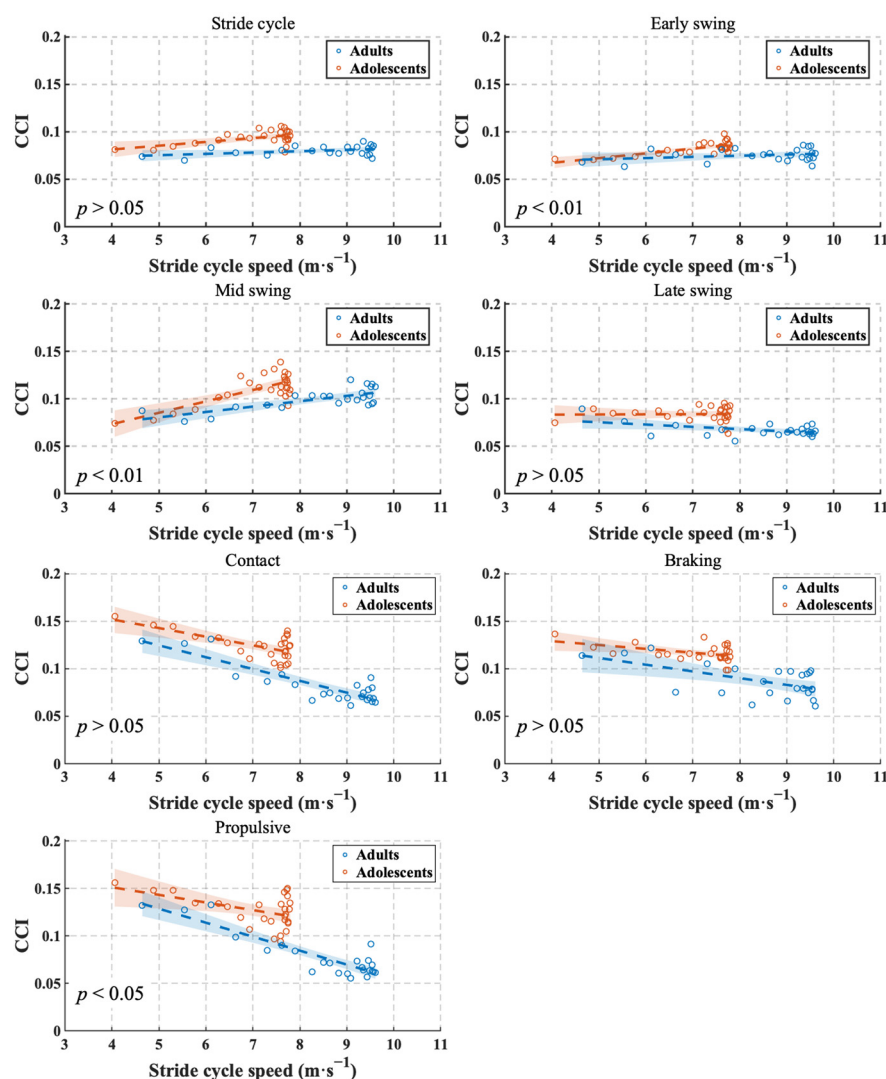


Figure 8. Relationship between stride cycle speed and BF-RF co-contraction index (CCI) across seven phases (stride cycle, early swing, mid swing, late swing, contact, braking, and propulsive) is shown using ordinary least squares (OLS) regression fitted to group mean values at each stride cycle. Points represent stride cycle-wise group mean values (averaged across participants) for both stride cycle frequency (x) and CCI (y), and dotted lines show OLS fits with 95% confidence bands (color shaded bands).

3.3.3. Akaike Information Criterion Analysis

Evidence for threshold-like behavior in the relationships between CCI and sprint variables was evaluated using AICc-based model comparisons. For stride cycle frequency, the piecewise model was best supported in Adults during mid swing, late swing, contact and propulsive phases, with breakpoints at 2.191–2.207 Hz. In Adolescents, the piecewise

model was best supported during contact and braking phases, with breakpoints at 2.106 Hz. In all remaining phases for both groups, the linear model was best supported and no breakpoint was retained. Full model-selection metrics (ΔAICc and Akaike weights) are provided in Table 8, and the corresponding AICc-selected fits with breakpoint locations (when supported) are visualized for all phases in Figure 9.

Table 8. Akaike Information Criterion (AICc) model-selection metrics for linear and single-breakpoint piecewise fits of the stride cycle frequency–CCI relationship across phases.

Group Name	Phase Name	ΔAICc (Linear)	Akaike Weights	Breakpoint (Hz)
Adults	Mid swing	0.94	0.62	2.19
	Late swing	6.52	0.96	2.21
	Contact	1.86	0.72	2.19
	Propulsive	4.83	0.92	2.21
Adolescents	Contact	0.83	0.60	2.11
	Braking	8.22	0.98	2.11

ΔAICc (linear – best) quantifies how much worse the linear model is relative to the best-supported model (0 indicates the linear model is best-supported). The Akaike weight for the piecewise model indicates its relative support among the candidate models. Breakpoints are reported only when the piecewise model is best supported.

For stride cycle speed, the piecewise model was best supported in Adults during late swing contact, braking and propulsive phases, with breakpoints at 6.106 to 9.510 $\text{m}\cdot\text{s}^{-1}$. In Adolescents, the piecewise model was best supported during stride cycle, mid swing, contact and propulsive phases, with breakpoints at 7.133 to 7.590 $\text{m}\cdot\text{s}^{-1}$. In all remaining phases for both groups, the linear model was best supported and no breakpoint was retained. Full model-selection metrics (ΔAICc and Akaike weights) are provided in Table 9, and the corresponding AICc-selected fits with breakpoint locations (when supported) are visualized for all phases in Figure 10.

Table 9. Akaike Information Criterion (AICc) model-selection metrics for linear and single-breakpoint piecewise fits of the stride cycle frequency–CCI relationship across phases.

Group Name	Phase Name	ΔAICc (Linear)	Akaike Weights	Breakpoint ($\text{m}\cdot\text{s}^{-1}$)
Adults	Late swing	12.67	1.00	6.11
	Contact	6.05	0.95	8.51
	Braking	0.54	0.58	9.51
	Propulsive	6.18	0.96	9.02
Adolescents	Stride cycle	1.33	0.66	7.13
	Mid swing	6.17	0.97	7.59
	Contact	4.77	0.92	7.58
	Propulsive	7.30	0.98	7.58

ΔAICc (linear – best) quantifies how much worse the linear model is relative to the best-supported model (0 indicates the linear model is best-supported). The Akaike weight for the piecewise model indicates its relative support among the candidate models. Breakpoints are reported only when the piecewise model is best supported.

3.4. Kinematics Data During Sprinting

Kinematic variables across the 50 m sprint are shown in Figures 11 and 12, and their descriptive statistics are summarized in Table 10. Figure 10 shows stride cycle speed, stride cycle length, and stride cycle frequency; Figure 11 shows contact time, braking time, propulsive time, relative braking time, and relative propulsive time (contact time = 100%).

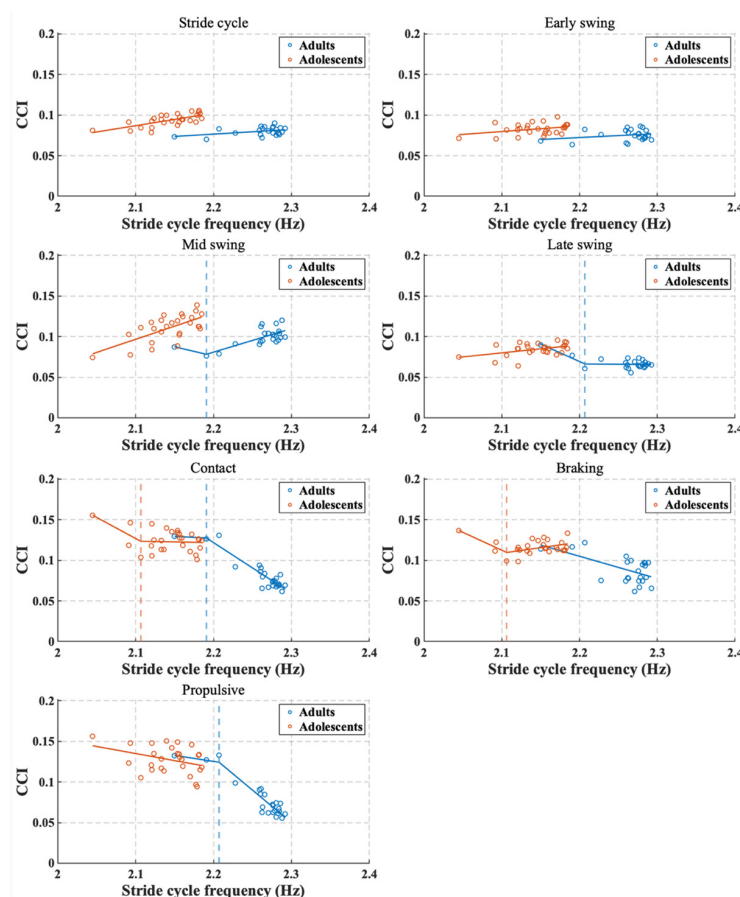


Figure 9. Akaike Information Criterion (AICc)-based breakpoint analysis of the relationship between stride cycle frequency and the BF–RF co-contraction index (CCI) across seven phases (stride cycle, early swing, mid swing, late swing, contact, braking, and propulsive). For each group and phase, linear and single-breakpoint segmented (piecewise) linear models were fitted to phase-specific group mean values at each stride cycle (one point per cycle). Solid lines show the best-supported model. Vertical dashed lines indicate the estimated breakpoint when the segmented model was best supported (Adults: blue; Adolescents: orange).

Table 10. Ground reaction force (GRF) data averaged the stride cycles in all participants.

Variables Name		Stride Cycle Speed (m·s ⁻¹)	Stride Cycle Length (m)	Stride Cycle Frequency (Hz)	Contact Time (s)	Braking Time (s)	Propulsive Time (s)	Braking Phase (%)	Propulsive Phase (%)
Adults	mean	8.52	3.77	2.26	0.11	0.03	0.08	29.44	70.97
	SD	1.24	0.51	0.03	0.02	0.01	0.03	11.09	11.14
Adolescents	mean	7.17	3.34	2.14	0.12	0.04	0.08	35.42	65.00
	SD	0.85	0.38	0.03	0.02	0.01	0.03	12.22	12.16

Data for each group are represented as mean and SD.

In Adults, stride cycle speed increased progressively and reached a plateau, with a peak at the 20th cycle ($9.544 \pm 0.405 \text{ m}\cdot\text{s}^{-1}$); from this peak to the final cycle (23rd cycle), the group mean speed decreased by 0.003%. Stride cycle frequency increased across cycles with only a slight late decline, peaking at the 12th cycle ($2.292 \pm 0.116 \text{ Hz}$) and decreasing by 1.344% by the final cycle. In Adolescents, stride cycle speed similarly increased and approached a plateau, peaking at the 20th cycle ($7.764 \pm 0.451 \text{ m}\cdot\text{s}^{-1}$); from this peak to the final cycle (27th cycle), the group mean speed decreased by 1.690%. Stride cycle frequency showed an early rise followed by a more pronounced decline, peaking at the 10th cycle ($2.185 \pm 0.080 \text{ Hz}$) and decreasing by 4.283% by the final cycle.

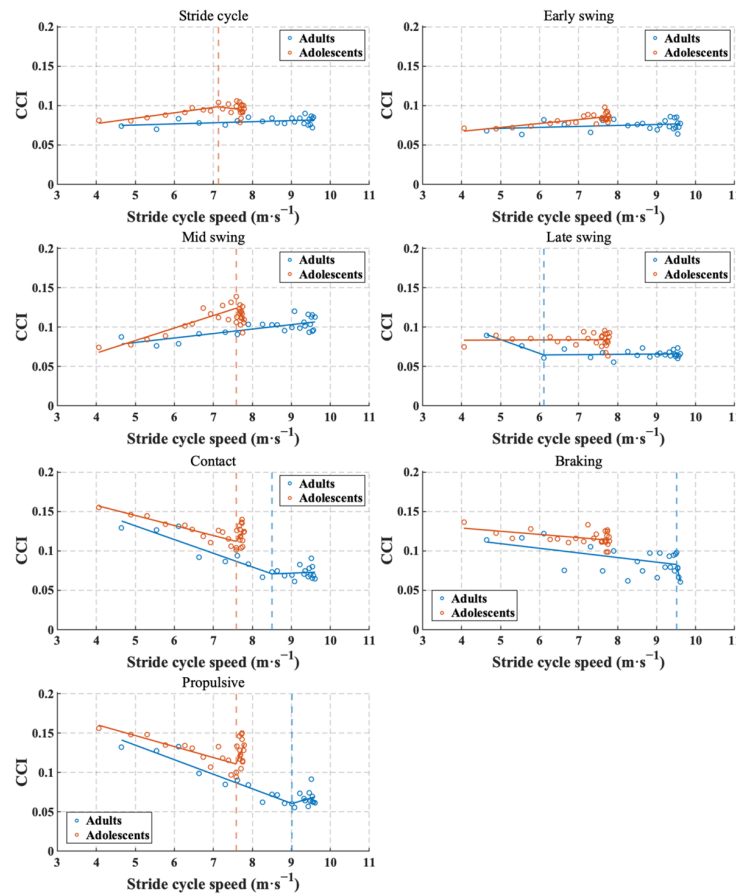


Figure 10. Akaike Information Criterion (AICc)-based breakpoint analysis of the relationship between stride cycle speed and the BF–RF co-contraction index (CCI) across seven phases (stride cycle, early swing, mid swing, late swing, contact, braking, and propulsive). For each group and phase, linear and single-breakpoint segmented (piecewise) linear models were fitted to phase-specific group mean values at each stride cycle (one point per cycle). Solid lines show the best-supported model. Vertical dashed lines indicate the estimated breakpoint when the segmented model was best supported (Adults: blue; Adolescents: orange).

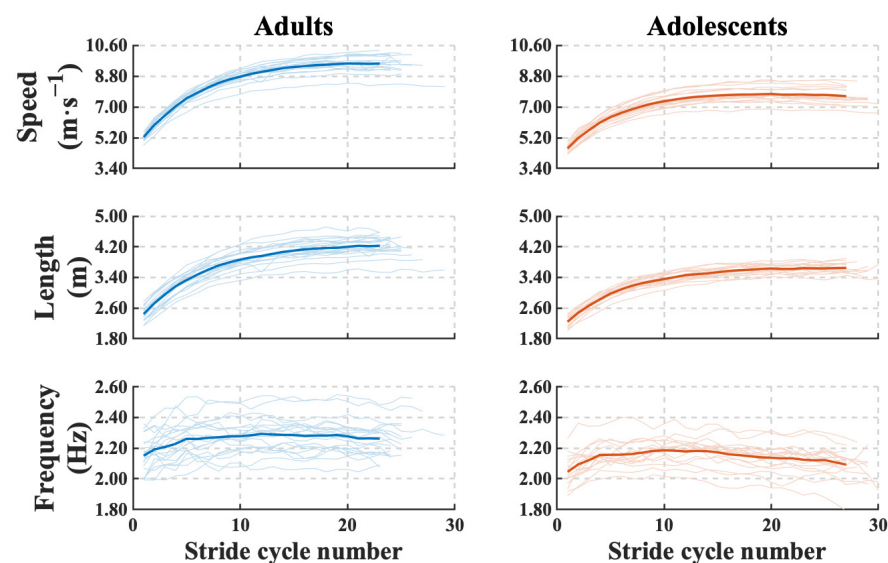


Figure 11. Ground reaction force (GRF) data across the stride cycles in all participants. Panels from top to bottom display stride cycle speed, length, and frequency. Group data are color-coded (Adults: blue; Adolescents: orange), where thick (or dark) lines represent the group means and thin (or light) lines represent individual participant data.

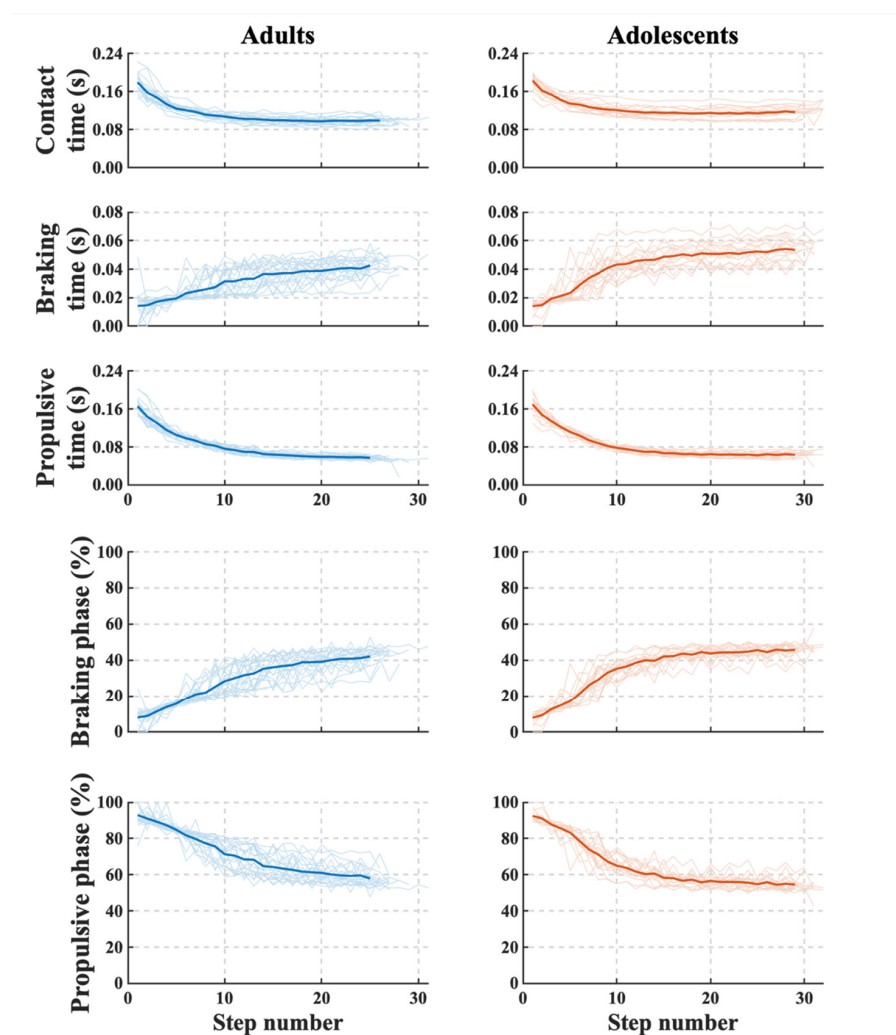


Figure 12. Ground reaction force (GRF) data across the stride cycles in all participants. The panels display contact time, braking time, propulsive time, relative braking time, and relative propulsive time. The color scheme and line representations are the same as in Figure 10.

4. Discussion

Our main findings were as follows: (1) Adolescents exhibited higher BF–RF co-contraction (CCI) than Adults during the contact and propulsive phases (bilaterally). (2) At the participant level (LME), between-group differences in the CCI–frequency association were observed in the stride cycle and late swing phases, whereas between-group differences in the CCI–speed association were observed in the mid swing phase ($x \times$ Group interaction). (3) At the group mean level (OLS; descriptive), the CCI–frequency relationship was more apparent in the stride cycle, late swing, contact, and braking phases, whereas the CCI–speed relationship was more apparent in the early swing, mid swing, and propulsive phases. (4) In the threshold-like behavior analysis (AICc), single-breakpoint piecewise models were supported in Adults for the CCI–frequency relationship during the mid swing, late swing, contact, and propulsive phases, and for the CCI–speed relationship during the late swing, contact, and braking phases. In Adolescents, piecewise support was observed for CCI–frequency during the contact and braking phases, and for CCI–speed during the stride cycle, mid swing, contact, and propulsive phases. These findings indicate age-related differences in neuromuscular coordination strategies during sprinting.

4.1. Relationship Between Phase-Specific Neuromuscular Coordination and Sprint Performance

In the late swing phase, between-group differences were not statistically significant; however, the observed small-to-moderate effect sizes (right: $g = 0.36$, left: $g = 0.52$) suggest that subtle age-related differences may exist. This late swing phase corresponds to the aerial period in which the lower limb swings posteriorly and is often referred to as “pawing.” Our previous work study a significant positive association between biceps femoris (BF) activity during late swing and sprint speed [10], and prior studies have also reported a positive relationship between sprint speed and posterior limb swing velocity [29]. Moreover, the late swing phase imposes substantial loads on the hamstrings [4–6,25,26]. In particular, BF muscle–tendon length is greatest during late swing phase, and the synchronization between peaks in muscle–tendon length and EMG activity suggests an elevated injury risk [34]. The observation that maximal-velocity sprinting exhibits greater knee extension than acceleration sprinting [6] is consistent with the possibility of increased stretch-related loading of the hamstring muscle–tendon unit during the late swing [34].

Co-contraction has been reported to increase with movement speed [15,21–24], and may be preferentially selected under conditions of heightened stabilization demands. Accordingly, increasing co-contraction with increasing sprint speed is reasonable, at least from a stabilization standpoint. In addition, youth are more likely to exhibit co-contraction during multi-joint dynamic tasks [2,11–13], and similar behavior may be expected during sprinting, even under high-load conditions such as late swing.

Across our analyses, adults tended to downregulate late-swing co-contraction as speed/frequency increased, whereas adolescents showed a relatively greater tendency toward frequency-/speed-dependent co-contraction. Taken together, these patterns suggest that, as loading demands rise with sprint speed/frequency, adults may shift toward a more reciprocal coordination strategy involving antagonist inhibition without a concomitant increase in CCI, whereas adolescents may rely more on co-contraction to stabilize the limb.

Prior work has reported that, during maximal sprinting, the thigh in Adolescents is positioned more posteriorly at toe-off [35], which may be related to prolonged hip extension and a tendency toward back-side mechanics. In the present study, Adolescents exhibited higher CCI during stance, with clearer age differences in the propulsive phase. Collectively, elevated co-contraction during the contact-phase may influence coordination in phases requiring rapid torque switching (i.e., hip extension → hip flexion), potentially disadvantaging limb repositioning and pitch maintenance. Indeed, delayed switching in BF–RF activation timing has been linked to reduced pitch [8], which is consistent with the tendency for adolescents to show a decline in stride cycle frequency toward the end of the sprint. Moreover, given that maturation has been suggested to increase feedforward activity and thereby improve performance [20], immature feedforward control in Adolescents may increase reliance on co-contraction for stabilization and, in turn, contribute to back-side mechanics.

Overall, Adolescents may increase CCI in a speed-dependent manner during the late swing, potentially supporting stabilization but also constraining pawing-related coordination and rapid extension–flexion switching. This could contribute to more pronounced back-side mechanics and a decline in stride cycle frequency in the latter part of the sprint.

During the contact and propulsive phases, Adolescents exhibited significantly higher bilateral CCI than Adults, and small-to-moderate effect sizes were observed in braking despite non-significant group differences. These findings support the interpretation that the ability to downregulate contact-phase co-contraction as speed/frequency increases may contribute to shorter contact times and more effective contact-phase mechanics. Because the neuromuscular system is still developing in Adolescents, factors such as immature sensitivity of muscle spindles and γ -motoneuron function [16], greater muscle–tendon

compliance [17], and relatively lower feedforward activity [20] may make pre-activation before ground contact less distinct than in Adults, contributing to age differences in contact-phase CCI. In other words, Adults may exhibit more proactive (feedforward-driven) activation patterns, whereas Adolescents may rely more on reactive (feedback-driven) patterns. This difference was most evident in the propulsive phase as defined in the present study (beginning at approximately 40 ms after foot contact).

4.2. Neuromuscular Function During Sprinting

High-rate force production depends on the recruitment of fast motor units [36], and the paw-shake response in cats has been shown to selectively recruit fast-type motor units [37]. Paw-shake is reported to emerge from interactions among spinal CPG output, segmental inertia, and viscoelastic muscle properties [38], and inter-segmental energy transfer can amplify oscillations in a whip-like manner [39]. Similar findings have been reported in humans, indicating the selective recruitment of fast-type motor units at high angular velocities [40,41].

In contrast, Adolescents have been reported to show a reduced capacity to utilize high-threshold motor units such as type II units [42,43], and they may exhibit lower activation of the motor unit pool than adults [44]. From a mechanical perspective, pawing may also contribute to propulsion via the whip-like amplification of inter-segmental energy transfer. However, considering age-related differences in muscle function, the speed-dependent increase in CCI during late swing in Adolescents may reflect a compensatory strategy prioritizing stabilization under conditions of insufficient high-threshold motor unit recruitment, thereby increasing reliance on co-contraction. Nevertheless, because motor unit activity was not measured in this study, this interpretation remains speculative.

During mid swing, CCI increased with speed and frequency in both groups, consistent with heightened stabilization demands during unilateral support while the contralateral limb is in contact. Interlimb reflex pathways may contribute to such interlimb coordination and dynamic stability. Interlimb reflexes have been suggested to play functional roles related to balance maintenance and fall avoidance [45–48]. Because sprinting involves repeated unilateral support at high speeds, the contribution of interlimb coordination mechanisms may be relatively larger. In particular, crossed reflex pathways mediated by commissural interneurons, where afferent input crosses within the spinal cord and projects to contralateral interneurons and motoneurons [49], may represent a plausible mechanism. Thus, the speed-dependent increase in CCI during mid swing could be explained by increased interlimb coordination demands accompanying heightened dynamic stability requirements. However, because interlimb reflexes were not measured in this study, this interpretation remains inconclusive.

Participation in youth sports has increased in recent years [50], and an increase in knee sprains—particularly ACL injuries—has been reported in adolescents, especially around 13–17 years of age [51]. Many noncontact ACL injuries occur during rapid deceleration tasks that include cutting and jump-landing maneuvers, where successful load management depends on anticipatory (feedforward) neuromuscular control and effective regulation of joint stiffness at or immediately before ground contact [52,53]. Consistent with this clinical framework, maturation-related changes in neuromuscular control and active joint stiffness have been documented across adolescence, suggesting that stabilization strategies may differ by developmental stage [54]. Notably, greater co-activation around the knee can increase joint stiffness and has been discussed as a potential protective strategy under destabilizing conditions [55]. In the present study, adolescents (13–15 years) exhibited higher CCI during contact-related phases than adults, which may reflect a greater reliance on stabilizing co-contraction during high-load sprint tasks. From an applied standpoint, these

phase-specific coordination patterns provide a mechanistic rationale for developmentally tailored neuromuscular training strategies aimed at optimizing stiffness regulation and reducing injury risk in youth athletes [52,56].

Adolescence encompasses rapid growth and maturation, and previous work indicates that neuromuscular function, muscle–tendon properties, and strength/power performance can change across maturation and around peak height velocity (PHV) [57,58]. In addition, sprint performance and its underlying spatiotemporal and mechanical determinants (e.g., changes in step length and contact time) have been reported to develop alongside maturation status and around the growth spurt, suggesting that maturation-related factors may influence running mechanics and, in turn, coordination demands during sprinting [59–61]. Although PHV (or other maturational indices such as maturity offset or Tanner stage) was not assessed in the present study, it is plausible that unmeasured maturation-related heterogeneity within the adolescent group contributed to inter-individual variability in phase-specific RF–BF coordination. Future studies incorporating maturational assessments (e.g., maturity offset/estimated age at PHV) could directly test whether phase-specific CCI patterns vary with maturation stage independent of chronological age.

4.3. Limitations

An a priori sample size calculation was not performed prior to data collection. To contextualize the adequacy of the final sample, we conducted a sensitivity analysis using G*Power 3.1 (two-tailed independent-samples *t* test, $\alpha = 0.05$, power = 0.80). With the final sample sizes (Adults: $n = 21$; Adolescents: $n = 17$), the minimum detectable standardized mean difference was Cohen's $d = 0.939$ (approximately equivalent to Hedges' $g \approx 0.919$ for $df = 36$). Therefore, the present study may have been underpowered to reliably detect small-to-moderate between-group effects, and nonsignificant findings should be interpreted with caution. Future studies with larger samples are warranted to confirm these findings and to detect more subtle effects. In addition, participants were recruited by convenience sampling from a single region, which may limit the generalizability of the findings to broader youth and adult athlete populations. Moreover, the sex distribution was imbalanced, particularly in the Adults group where the number of female participants was small. Therefore, sex-stratified analyses were not feasible, and potential sex-related differences in phase-specific neuromuscular coordination could not be evaluated; the present findings should not be overgeneralized across sexes. As a robustness check, we repeated the primary between-group comparisons after excluding the single female participant in the adult group; the overall pattern of results and effect sizes was materially similar, although the contact phase for the right leg shifted from statistically significant to borderline ($p = 0.06$, $g = 0.63$), while significant differences remained for contact on the left ($p < 0.05$, $g = 0.84$) and for the propulsive phase on both legs (right: $p < 0.05$, $g = 0.71$; left: $p < 0.05$, $g = 0.83$).

A methodological limitation is that sEMG may be affected by crosstalk from adjacent muscles, particularly in the thigh where muscles are anatomically close; therefore, the present EMG results should be interpreted as reflecting activity within the recording region rather than perfectly isolated muscle activation. In addition, within-session reliability of the MVC measurements used for EMG normalization was not formally quantified (e.g., test–retest ICC or coefficient of variation). Although MVC trials were performed using a standardized protocol, this may introduce uncertainty in %MVC scaling and should be addressed in future studies.

The Adolescents studied here were junior high school track-and-field athletes training at least twice per week for two hours per session and therefore do not represent a sedentary adolescent population. Although the present design cannot disentangle whether the observed age differences in phase-specific neuromuscular coordination reflect maturation

or training experience, the findings indicate that such differences can be present even in Adolescents engaged in competitive-level training, and may provide useful insights for understanding sprint-specific skill acquisition. Because motor unit behavior and reflex mechanisms were not directly measured, mechanistic interpretations regarding maturation-related changes in neuromuscular control should be considered indirect.

Future studies should clarify whether the main phase-specific age differences observed here are primarily maturation-related or attributable to training experience. In addition, because some Adolescents exhibited adult-like coordination patterns (and vice versa), further analyses are warranted to characterize individual variability in neuromuscular control strategies and to identify features of participants who deviate from typical group patterns.

5. Conclusions

This study demonstrated phase-specific age differences in agonist–antagonist coordination of the biarticular thigh muscles during 50 m sprinting. Adolescents showed greater bilateral BF–RF co-contraction during contact and propulsion, and age differences in the CCI–frequency slope (OLS) were largest in these phases. In contrast, adults generally downregulated co-contraction as speed/frequency increased, and model selection supported threshold-like behavior in multiple phases, consistent with a transition toward more reciprocal coordination under higher demand. Overall, these findings suggest that adolescents rely more on stabilizing co-contraction under comparable sprint demands, whereas adults more effectively modulate co-contraction with increasing speed/frequency. These results provide a rationale for age informed training design and injury prevention considerations in developing athletes.

Author Contributions: Conceptualization, K.Y. and H.T.; methodology, K.Y. and H.T.; software, K.Y.; formal analysis, K.Y.; validation, K.Y.; investigation, K.Y.; resources, K.Y. and H.T.; data curation, K.Y.; writing—original draft preparation, K.Y.; writing—review and editing, H.T.; visualization, K.Y.; supervision, H.T.; funding acquisition, K.Y. and H.T.; project administration, H.T. All authors have read and agreed to the published version of the manuscript.

Funding: This work was supported by Japan Science and Technology Agency Support for Pioneering Research Initiated by the Next Generation—JST SPRING (Grant Number JPMJSP2164).

Institutional Review Board Statement: The study was conducted in accordance with the Declaration of Helsinki and approved by the research ethics committee of the National Institute of Fitness and Sports in Kanoya (25-1-37).

Informed Consent Statement: Informed consent was obtained from all participants involved in the study.

Data Availability Statement: Data are contained within the article; please contact the authors if you need anything else.

Acknowledgments: We would like to thank the participants who contributed their time and data to our study. We would also like to thank the faculty, staff, and students of the SPORTEC Sports Performance Research Center for their assistance with facility management and support in utilizing the research environment.

Conflicts of Interest: The authors declare no conflicts of interest.

References

1. Rudolph, K.S.; Axe, M.J.; Snyder-Mackler, L. Dynamic stability after ACL injury: Who can hop? *Knee Surg. Sports Traumatol. Arthrosc.* **2000**, *8*, 262–269. [[CrossRef](#)] [[PubMed](#)]
2. Dotan, R.; Mitchell, C.; Cohen, R.; Klentrou, P.; Gabriel, D.; Falk, B. Child-adult differences in muscle activation—A review. *Pediatr. Exerc. Sci.* **2012**, *24*, 2–21. [[CrossRef](#)] [[PubMed](#)]

3. Williams, J.J.; Roshinski, W.C.; Watso, J.C. Upper Leg Muscular Co-Contraction During Maximal-Speed Sprinting in Male Club Ice Hockey Athletes. *Sports Med. Open* **2025**, *11*, 1. [[CrossRef](#)] [[PubMed](#)]
4. Schache, A.G.; Kim, H.J.; Morgan, D.L.; Pandy, M.G. Hamstring muscle forces prior to and immediately following an acute sprinting-related muscle strain injury. *Gait Posture* **2010**, *32*, 136–140. [[CrossRef](#)]
5. Schache, A.G.; Blanch, P.D.; Dorn, T.W.; Brown, N.A.; Rosemond, D.; Pandy, M.G. Effect of running speed on lower limb joint kinetics. *Med. Sci. Sports Exerc.* **2011**, *43*, 1260–1271. [[CrossRef](#)]
6. Higashihara, A.; Nagano, Y.; Ono, T.; Fukubayashi, T. Differences in hamstring activation characteristics between the acceleration and maximum-speed phases of sprinting. *J. Sports Sci.* **2018**, *36*, 1313–1318. [[CrossRef](#)]
7. Kakehata, G.; Goto, Y.; Iso, S.; Kanosue, K. Timing of Rectus Femoris and Biceps Femoris Muscle Activities in Both Legs at Maximal Running Speed. *Med. Sci. Sports Exerc.* **2021**, *53*, 643–652. [[CrossRef](#)]
8. Kakehata, G.; Goto, Y.; Iso, S.; Kanosue, K. The Timing of Thigh Muscle Activity Is a Factor Limiting Performance in the Deceleration Phase of the 100-m Dash. *Med. Sci. Sports Exerc.* **2022**, *54*, 1002–1012. [[CrossRef](#)]
9. Kakehata, G.; Goto, Y.; Yokoyama, H.; Iso, S.; Kanosue, K. Interlimb and Intralimb Coordination of Rectus Femoris and Biceps Femoris Muscles at Different Running Speeds. *Med. Sci. Sports Exerc.* **2023**, *55*, 945–956. [[CrossRef](#)]
10. Yokota, K.; Tamaki, H. Application of Wireless EMG Sensors for Assessing Agonist-Antagonist Muscle Activity During 50-m Sprinting in Athletes. *Sensors* **2025**, *25*, 6395. [[CrossRef](#)]
11. Geertsen, S.S.; Willerslev-Olsen, M.; Lorentzen, J.; Nielsen, J.B. Development and aging of human spinal cord circuitries. *J. Neurophysiol.* **2017**, *118*, 1133–1140. [[CrossRef](#)]
12. Radnor, J.M.; Oliver, J.L.; Waugh, C.M.; Myer, G.D.; Moore, I.S.; Lloyd, R.S. The Influence of Growth and Maturation on Stretch-Shortening Cycle Function in Youth. *Sports Med.* **2018**, *48*, 57–71. [[CrossRef](#)] [[PubMed](#)]
13. Woods, S.; O'Mahoney, C.; McKiel, A.; Natale, L.; Falk, B. Child-Adult differences in antagonist muscle coactivation: A systematic review. *J. Electromyogr. Kinesiol.* **2023**, *68*, 102727. [[CrossRef](#)]
14. De Luca, C.J.; Mambrito, B. Voluntary control of motor units in human antagonist muscles: Coactivation and reciprocal activation. *J. Neurophysiol.* **1987**, *58*, 525–542. [[CrossRef](#)]
15. Baratta, R.; Solomonow, M.; Zhou, B.H.; Letson, D.; Chuinard, R.; D'Ambrosia, R. Muscular coactivation. The role of the antagonist musculature in maintaining knee stability. *Am. J. Sports Med.* **1988**, *16*, 113–122. [[CrossRef](#)]
16. Grosset, J.F.; Mora, I.; Lambert, D.; Perot, C. Changes in stretch reflexes and muscle stiffness with age in prepubescent children. *J. Appl. Physiol.* **2007**, *102*, 2352–2360. [[CrossRef](#)]
17. Lazaridis, S.; Bassa, E.; Patikas, D.; Giakas, G.; Gollhofer, A.; Kotzamanidis, C. Neuromuscular differences between prepubescent boys and adult men during drop jump. *Eur. J. Appl. Physiol.* **2010**, *110*, 67–74. [[CrossRef](#)]
18. Oliver, J.L.; Smith, P.M. Neural control of leg stiffness during hopping in boys and men. *J. Electromyogr. Kinesiol.* **2010**, *20*, 973–979. [[CrossRef](#)] [[PubMed](#)]
19. Horita, T.; Komi, P.V.; Nicol, C.; Kyrolainen, H. Interaction between pre-landing activities and stiffness regulation of the knee joint musculoskeletal system in the drop jump: Implications to performance. *Eur. J. Appl. Physiol.* **2002**, *88*, 76–84. [[CrossRef](#)]
20. Lloyd, R.S.; Oliver, J.L.; Hughes, M.G.; Williams, C.A. Age-related differences in the neural regulation of stretch-shortening cycle activities in male youths during maximal and sub-maximal hopping. *J. Electromyogr. Kinesiol.* **2012**, *22*, 37–43. [[CrossRef](#)] [[PubMed](#)]
21. Lestienne, F. Effects of inertial load and velocity on the braking process of voluntary limb movements. *Exp. Brain Res.* **1979**, *35*, 407–418. [[CrossRef](#)]
22. Smith, A.M. The coactivation of antagonist muscles. *Can. J. Physiol. Pharmacol.* **1981**, *59*, 733–747. [[CrossRef](#)] [[PubMed](#)]
23. Benecke, R.; Meinck, H.M.; Conrad, B. Rapid goal-directed elbow flexion movements: Limitations of the speed control system due to neural constraints. *Exp. Brain Res.* **1985**, *59*, 470–477. [[CrossRef](#)]
24. Kido, A.; Tanaka, N.; Stein, R.B. Spinal reciprocal inhibition in human locomotion. *J. Appl. Physiol.* **2004**, *96*, 1969–1977. [[CrossRef](#)]
25. Thelen, D.G.; Chumanov, E.S.; Best, T.M.; Swanson, S.C.; Heiderscheid, B.C. Simulation of biceps femoris musculotendon mechanics during the swing phase of sprinting. *Med. Sci. Sports Exerc.* **2005**, *37*, 1931–1938. [[CrossRef](#)]
26. Chumanov, E.S.; Heiderscheid, B.C.; Thelen, D.G. The effect of speed and influence of individual muscles on hamstring mechanics during the swing phase of sprinting. *J. Biomech.* **2007**, *40*, 3555–3562. [[CrossRef](#)] [[PubMed](#)]
27. Schache, A.G.; Dorn, T.W.; Blanch, P.D.; Brown, N.A.; Pandy, M.G. Mechanics of the human hamstring muscles during sprinting. *Med. Sci. Sports Exerc.* **2012**, *44*, 647–658. [[CrossRef](#)]
28. Higashihara, A.; Ono, T.; Kubota, J.; Okuwaki, T.; Fukubayashi, T. Functional differences in the activity of the hamstring muscles with increasing running speed. *J. Sports Sci.* **2010**, *28*, 1085–1092. [[CrossRef](#)] [[PubMed](#)]
29. Mattes, K.; Wolff, S.; Alizadeh, S. Kinematic Stride Characteristics of Maximal Sprint Running of Elite Sprinters—Verification of the “Swing-Pull Technique”. *J. Hum. Kinet.* **2021**, *77*, 15–24. [[CrossRef](#)]
30. Hermens, H.J.; Freriks, B.; Disselhorst-Klug, C.; Rau, G. Development of recommendations for SEMG sensors and sensor placement procedures. *J. Electromyogr. Kinesiol.* **2000**, *10*, 361–374. [[CrossRef](#)]

31. Knarr, B.A.; Zeni, J.A., Jr.; Higginson, J.S. Comparison of electromyography and joint moment as indicators of co-contraction. *J. Electromyogr. Kinesiol.* **2012**, *22*, 607–611. [[CrossRef](#)] [[PubMed](#)]
32. Kubota, K.; Yokoyama, M.; Hanawa, H.; Miyazawa, T.; Hirata, K.; Onitsuka, K.; Fujino, T.; Kanemura, N. Muscle co-activation in the elderly contributes to control of hip and knee joint torque and endpoint force. *Sci. Rep.* **2023**, *13*, 7139. [[CrossRef](#)] [[PubMed](#)]
33. Li, G.; Shourijeh, M.S.; Ao, D.; Patten, C.; Fregly, B.J. How Well Do Commonly Used Co-contraction Indices Approximate Lower Limb Joint Stiffness Trends During Gait for Individuals Post-stroke? *Front. Bioeng. Biotechnol.* **2020**, *8*, 588908. [[CrossRef](#)]
34. Higashihara, A.; Nagano, Y.; Ono, T.; Fukubayashi, T. Relationship between the peak time of hamstring stretch and activation during sprinting. *Eur. J. Sport Sci.* **2016**, *16*, 36–41. [[CrossRef](#)]
35. Chatzilazaridis, I.; Panoutsakopoulos, V.; Bassa, E.; Kotzamanidou, M.C.; Papaikakou, G.I. Effects of Age and Sex on the Kinematics of the Sprinting Technique in the Maximum Velocity Phase. *Appl. Sci.* **2024**, *14*, 6057. [[CrossRef](#)]
36. Claffin, D.R.; Faulkner, J.A. Shortening velocity extrapolated to zero load and unloaded shortening velocity of whole rat skeletal muscle. *J. Physiol.* **1985**, *359*, 357–363. [[CrossRef](#)]
37. Smith, J.L.; Betts, B.; Edgerton, V.R.; Zernicke, R.F. Rapid ankle extension during paw shakes: Selective recruitment of fast ankle extensors. *J. Neurophysiol.* **1980**, *43*, 612–620. [[CrossRef](#)]
38. Prilutsky, B.I.; Parker, J.; Cymbalyuk, G.S.; Klishko, A.N. Emergence of Extreme Paw Accelerations During Cat Paw Shaking: Interactions of Spinal Central Pattern Generator, Hindlimb Mechanics and Muscle Length-Depended Feedback. *Front. Integr. Neurosci.* **2022**, *16*, 810139. [[CrossRef](#)]
39. Hoy, M.G.; Zernicke, R.F.; Smith, J.L. Contrasting roles of inertial and muscle moments at knee and ankle during paw-shake response. *J. Neurophysiol.* **1985**, *54*, 1282–1294. [[CrossRef](#)] [[PubMed](#)]
40. Nardone, A.; Romano, C.; Schieppati, M. Selective recruitment of high-threshold human motor units during voluntary isotonic lengthening of active muscles. *J. Physiol.* **1989**, *409*, 451–471. [[CrossRef](#)] [[PubMed](#)]
41. Tamaki, H.; Kitada, K.; Akamine, T.; Sakou, T.; Kurata, H. Electromyogram patterns during plantarflexions at various angular velocities and knee angles in human triceps surae muscles. *Eur. J. Appl. Physiol. Occup. Physiol.* **1997**, *75*, 1–6. [[CrossRef](#)]
42. Falk, B.; Dotan, R. Child-adult differences in the recovery from high-intensity exercise. *Exerc. Sport Sci. Rev.* **2006**, *34*, 107–112. [[CrossRef](#)] [[PubMed](#)]
43. Falk, B.; Usselman, C.; Dotan, R.; Brunton, L.; Klentrou, P.; Shaw, J.; Gabriel, D. Child-adult differences in muscle strength and activation pattern during isometric elbow flexion and extension. *Appl. Physiol. Nutr. Metab.* **2009**, *34*, 609–615. [[CrossRef](#)]
44. Woods, S.; O'Mahoney, C.; Maynard, J.; Dotan, R.; Tenenbaum, G.; Filho, E.; Falk, B. Increase in Volitional Muscle Activation from Childhood to Adulthood: A Systematic Review and Meta-analysis. *Med. Sci. Sports Exerc.* **2022**, *54*, 789–799. [[CrossRef](#)] [[PubMed](#)]
45. Gervasio, S.; Farina, D.; Sinkjaer, T.; Mrachacz-Kersting, N. Crossed reflex reversal during human locomotion. *J. Neurophysiol.* **2013**, *109*, 2335–2344. [[CrossRef](#)]
46. Stevenson, A.J.; Geertsen, S.S.; Andersen, J.B.; Sinkjaer, T.; Nielsen, J.B.; Mrachacz-Kersting, N. Interlimb communication to the knee flexors during walking in humans. *J. Physiol.* **2013**, *591*, 4921–4935. [[CrossRef](#)]
47. Gervasio, S.; Kersting, U.G.; Farina, D.; Mrachacz-Kersting, N. The effect of crossed reflex responses on dynamic stability during locomotion. *J. Neurophysiol.* **2015**, *114*, 1034–1040. [[CrossRef](#)]
48. Stevenson, A.J.; Geertsen, S.S.; Sinkjaer, T.; Nielsen, J.B.; Mrachacz-Kersting, N. Interlimb communication following unexpected changes in treadmill velocity during human walking. *J. Neurophysiol.* **2015**, *113*, 3151–3158. [[CrossRef](#)]
49. Stevenson, A.J.; Kamavuako, E.N.; Geertsen, S.S.; Farina, D.; Mrachacz-Kersting, N. Short-latency crossed responses in the human biceps femoris muscle. *J. Physiol.* **2015**, *593*, 3657–3671. [[CrossRef](#)]
50. Logan, K.; Cuff, S.; Council on Sports Medicine and Fitness. Organized Sports for Children, Preadolescents, and Adolescents. *Pediatrics* **2019**, *143*, e20190997. [[CrossRef](#)] [[PubMed](#)]
51. Turati, M.; Benedettini, E.; Sugimoto, D.; Crippa, M.; Alessandro, C.; Bacchin, V.; Piatti, M.; Albanese, F.; Accadbled, F.; Rigamonti, L.; et al. Quadriceps and hamstring muscles strength differences in adolescent and adult recreational athletes 6 months after autograft bone-patellar-tendon-bone anterior cruciate ligament reconstruction: A retrospective study. *Knee* **2025**, *54*, 9–18. [[CrossRef](#)]
52. Di Stasi, S.; Myer, G.D.; Hewett, T.E. Neuromuscular training to target deficits associated with second anterior cruciate ligament injury. *J. Orthop. Sports Phys. Ther.* **2013**, *43*, 777–792, A1–A11. [[CrossRef](#)]
53. Bencke, J.; Aagaard, P.; Zebis, M.K. Muscle Activation During ACL Injury Risk Movements in Young Female Athletes: A Narrative Review. *Front. Physiol.* **2018**, *9*, 445. [[CrossRef](#)] [[PubMed](#)]
54. Ford, K.R.; Myer, G.D.; Hewett, T.E. Longitudinal effects of maturation on lower extremity joint stiffness in adolescent athletes. *Am. J. Sports Med.* **2010**, *38*, 1829–1837. [[CrossRef](#)]
55. Ramezani, F.; Saki, F.; Tahayori, B. Neuromuscular training improves muscle co-activation and knee kinematics in female athletes with high risk of anterior cruciate ligament injury. *Eur. J. Sport Sci.* **2024**, *24*, 56–65. [[CrossRef](#)]

56. Ramachandran, A.K.; Pedley, J.S.; Moeskops, S.; Oliver, J.L.; Myer, G.D.; Hsiao, H.I.; Lloyd, R.S. Influence of Neuromuscular Training Interventions on Jump-Landing Biomechanics and Implications for ACL Injuries in Youth Females: A Systematic Review and Meta-analysis. *Sports Med.* **2025**, *55*, 1265–1292. [[CrossRef](#)] [[PubMed](#)]
57. Tumkur Anil Kumar, N.; Oliver, J.L.; Lloyd, R.S.; Pedley, J.S.; Radnor, J.M. The Influence of Growth, Maturation and Resistance Training on Muscle-Tendon and Neuromuscular Adaptations: A Narrative Review. *Sports* **2021**, *9*, 59. [[CrossRef](#)] [[PubMed](#)]
58. Retzepis, N.O.; Avloniti, A.; Kokkotis, C.; Stampoulis, T.; Balampanos, D.; Gkachtsou, A.; Aggelakis, P.; Kelaraki, D.; Protopapa, M.; Pantazis, D.; et al. The Effect of Peak Height Velocity on Strength and Power Development of Young Athletes: A Scoping Review. *J. Funct. Morphol. Kinesiol.* **2025**, *10*, 168. [[CrossRef](#)]
59. Meyers, R.W.; Oliver, J.L.; Hughes, M.G.; Cronin, J.B.; Lloyd, R.S. Maximal sprint speed in boys of increasing maturity. *Pediatr. Exerc. Sci.* **2015**, *27*, 85–94. [[CrossRef](#)]
60. Moran, J.; Parry, D.A.; Lewis, I.; Collison, J.; Rumpf, M.C.; Sandercock, G.R.H. Maturation-related adaptations in running speed in response to sprint training in youth soccer players. *J. Sci. Med. Sport.* **2018**, *21*, 538–542. [[CrossRef](#)]
61. Okudaira, M.; Takeda, R.; Hirono, T.; Nishikawa, T.; Kunugi, S.; Igawa, K.; Ueda, S.; Mita, Y.; Watanabe, K. Determinants of Sprint Ability Change During Maturation in Developing Children. *Eur. J. Sport Sci.* **2026**, *26*, e70133. [[CrossRef](#)] [[PubMed](#)]

Disclaimer/Publisher’s Note: The statements, opinions and data contained in all publications are solely those of the individual author(s) and contributor(s) and not of MDPI and/or the editor(s). MDPI and/or the editor(s) disclaim responsibility for any injury to people or property resulting from any ideas, methods, instructions or products referred to in the content.